Korea-Australia Rheology Journal, 27(4), 267-285 (November 2015) www.springer.com/13367
DOI: 10.1007/s13367-015-0027-7

Reflections on inflections

C. Saengow[1,3], A.J. Giacomin[1,2,*], P.H. Gilbert[1] and C. Kolitawong[3]
[1]*Chemical Engineering Department and Polymers Research Group*
[2]*Mechanical and Materials Engineering Department, Queen's University, Kingston, Ontario, Canada K7L 3N6*
[3]*Mechanical and Aerospace Engineering Department, Polymer Research Center, King Mongkut's University of Technology North Bangkok, Bangkok, Thailand 10800*

(Received July 15, 2015; final revision received October 20, 2015; accepted October 22, 2015)

In plastics processing, the single most important rheological property is the steady shear *viscosity curve*: the logarithm of the steady shear viscosity versus the logarithm of the shear rate. This curve governs the volumetric flowrate through any straight channel flow, and thus governs the production rate of extruded plastics. If the shear rate is made dimensionless with a characteristic time for the fluid (called the Weissenberg number, Wi), then we can readily identify the end of the Newtonian plateau of a viscosity curve with the value $\mathrm{Wi} \approx 1$. Of far greater importance, however, is the *slope* at the point where the viscosity curve inflects, (n–1), where n is called the *shear power-law index*. This paper explores the physics of this point and related inflections, in the first and second normal stress coefficients. We also discuss the first and second *inflection pairing times*, λ'_{B} and λ''_{B}. First, we examine the generalized Newtonian fluid (Carreau model). Then, we analyze the more versatile model, the corotational Oldroyd 8-constant model, which reduces to many simpler models, for instance, the corotational Maxwell and Jeffreys models. We also include worked examples to illustrate the procedure for calculating inflection points and power-law coefficients for all three viscometric functions, $\eta(\dot{\gamma})$, $\Psi_1(\dot{\gamma})$ and $\Psi_2(\dot{\gamma})$.

Keywords: steady shear flow, viscosity curve, viscosity inflection, normal stress coefficients, normal stress differences

1. Introduction

In plastics processing, the single most important rheological property is the *steady shear viscosity curve*: the logarithm of the steady shear viscosity *versus* the logarithm of the shear rate. This curve governs, for instance, the volumetric flowrate through any straight channel flow, and thus determines the production rate of extruded plastics. If the shear rate is made dimensionless with a characteristic time for the fluid, we call the result the *Weissenberg number*, Wi. We can readily, and generally, identify the end of the Newtonian plateau of a viscosity curve with the value $\mathrm{Wi} \approx 1$. In other words, we associate a characteristic time, λ, with the "roll-off" value of the Weissenberg number, $\mathrm{Wi}_{\mathrm{N}} \equiv \lambda \dot{\gamma}_{\mathrm{N}} \approx 1$ (where $\dot{\gamma}_{\mathrm{N}}$ is the roll-off steady shear rate). For example, for the Carreau model, λ_C is the reciprocal of the roll-off shear rate. Of far greater commercial importance, however, is the *slope* where the viscosity curve inflects, (n–1), where n is called the *shear power-law index*, and about which, little is written. In this connection, we know of no textbook treatment of viscosity curve inflection. Clearly, with the viscosity inflection at Wi_{i}, we identify an *inflection characteristic time*, λ_{i}. We thus call λ the *roll-off characteristic time* of the fluid. This paper explores the physics of this and two related inflections which are the first and second normal stress coefficients, by deriving expressions for this slope from two constitutive equations: one generalized Newtonian (Carreau) and one corotational viscoelastic (Oldroyd 8-constant) which can be reduced to many simpler models [see Eq. (36) ff in Saengow *et al.* (2015a and b); Table 8.1-1 in Bird *et al.* (1977); Table 7.3-2 in Bird *et al.* (1987)] in Subsection 3.1 and 3.2.

Of course, where the viscosity curve approaches the second Newtonian plateau at the *second Weissenberg number*, Wi_{∞}, we identify the *second characteristic time*, λ_{∞}, which lies beyond the scope of our reflections on inflections. For fluids with a first normal stress coefficient, $\Psi_1(\dot{\gamma})$, we identify an additional set of three characteristic times, λ', λ'_{i} and λ'_{∞}, which we, of course, expect to relate to λ, λ_{i} and λ_{∞}. For fluids with a second normal stress coefficient, $\Psi_2(\dot{\gamma})$, we identify an additional set of three characteristic times, λ'', λ''_{i} and λ''_{∞}, which we again expect to relate to λ, λ_{i} and λ_{∞}. By now, the reader will have noticed that, in this paper, we use primes for quantities related to $\Psi_1(\dot{\gamma})$, and double primes for those related to $\Psi_2(\dot{\gamma})$. In this work, we define every symbol, dimensional in Table 1, and dimensionless, in Table 2.

With each inflection, we associate a tangent [Eq. (5.2-53) in Bird *et al.* (1977)]:

$$\eta(\dot{\gamma}) = m\dot{\gamma}^{n-1} \tag{1}$$

*Corresponding author; E-mail: giacomin@queensu.ca

Table 1. Dimensional variables.

Name	Unit	Symbol	Eq.
Any coordinates, *i*-th	L	x_i	
Carreau characteristic time, first normal	t	λ_C'	(7)
Carreau characteristic time, second normal	t	λ_C''	(8)
Carreau characteristic time, shear	t	λ_C	(6)
Coefficient in Eq. (115)	t	α	(115)
Coefficient in Eq. (116)	t	β	(116)
Coefficient in Eq. (139)	t	A	(139)
Coefficient in Eq. (140)	t	B	(140)
Corotational derivative	t^{-1}	$\frac{\mathscr{D}}{\mathscr{D}t}$	(12)
Extra stress tensor*	M/Lt^2	$\boldsymbol{\tau}$	(9)
First normal stress coefficient	M/L	$\Psi_1 \equiv -(\tau_{11}-\tau_{22})/\dot{\gamma}^2$	
First normal stress coefficient, infinite shear rate	M/L	$\Psi_{1\infty} \equiv \lim_{\dot{\gamma}\to\infty}\Psi_1$	
First normal stress coefficient, inflection	M/L	Ψ_{1i}	
First normal stress coefficient, *k*-th spectrum	M/L	Ψ_{1k}	(205)
First normal stress coefficient, zero shear rate	M/L	$\Psi_{10} \equiv \lim_{\dot{\gamma}\to 0}\Psi_1$	
Inflection characteristic time, first normal	t	λ_i'	
Inflection characteristic time, second normal	t	λ_i''	
Inflection characteristic time, shear	t	λ_i	
Oldroyd coefficient	t	μ_0	(9)
Oldroyd coefficient	t	μ_1	(9)
Oldroyd coefficient	t	μ_2	(9)
Oldroyd coefficient	t	ν_1	(9)
Oldroyd coefficient	t	ν_2	(9)
Oldroyd coefficient, relaxation time	t	λ_1	(9)
Oldroyd coefficient, relaxation time, *k*-th spectrum	t	λ_{1k}	(181)
Oldroyd coefficient, retardation time	t	λ_2	(9)
Oldroyd coefficient, retardation time, *k*-th spectrum	t	λ_{2k}	(182)
Oldroyd shear thickening constant	t^2	σ_2	(16)
Oldroyd shear thickening constant, *n*-th specturm	t^2	σ_{2n}	
Oldroyd shear thinning constant	t^2	σ_1	(15)
Oldroyd shear thinning constant, *n*-th spectrum	t^2	σ_{1n}	(92)
Pairing time, first inflection	t	λ_B'	(4)
Pairing time, second inflection	t	λ_B''	(5)
Power-law coefficient, first normal	M/Lt^{2-n}	m'	(44)
Power-law coefficient, second normal	M/Lt^{2-n}	m''	(45)
Power-law coefficient, shear	M/Lt^{2-n}	m	(43)
Rate-of-deformation tensor	t^{-1}	$\dot{\boldsymbol{\gamma}} \equiv \nabla\mathbf{v} + (\nabla\mathbf{v})^\dagger$	(11)
Roll-off characteristic time, first normal	t	λ'	
Roll-off characteristic time, second normal	t	λ''	
Roll-off characteristic time, shear	t	λ	
Second characteristic time, first normal stress coefficient	t	λ_∞'	
Second characteristic time, second normal stress	t	λ_∞''	
Second characteristic time, steady shear viscosity	t	λ_∞	
Second normal stress coefficient	M/L	$\Psi_2 \equiv -(\tau_{22}-\tau_{33})/\dot{\gamma}^2$	
Second normal stress coefficient, infinite shear rate	M/L	$\Psi_{2\infty} \equiv \lim_{\dot{\gamma}\to\infty}\Psi_2$	
Second normal stress coefficient, inflection	M/L	Ψ_{2i}	
Second normal stress coefficient, zero shear rate	M/L	$\Psi_{20} \equiv \lim_{\dot{\gamma}\to 0}\Psi_2$	
Shear rate, *yx*-component, steady	t^{-1}	$\dot{\gamma}$	
Shear rate, *yx*-component, steady, inflection	t^{-1}	$\dot{\gamma}_i$	
Shear rate, *yx*-component, roll-off	t^{-1}	$\dot{\gamma}_N$	

Table 1. Continued.

Name	Unit	Symbol	Eq.
Steady shear viscosity	M/Lt	η	(14)
Steady shear viscosity, infinite shear rate	M/Lt	η_∞	
Steady shear viscosity, inflection	M/Lt	η_i	(90)
Steady shear viscosity, k-th spectrum	M/Lt	η_k	(180)
Steady shear viscosity, zero shear rate	M/Lt	η_0	(9)
Total stress tensor	M/Lt^2	$\boldsymbol{\pi} \equiv \boldsymbol{\tau} + p\boldsymbol{\delta}$	(10)
Time	t	t	(165)
Time, polymer processing characteristic	t	t_p	(165)
Vorticity tensor	t^{-1}	$\boldsymbol{\omega} \equiv \nabla\mathbf{v} - (\nabla\mathbf{v})^\dagger$	(13)

Legend: $M \equiv$ mass; $L \equiv$ length; $t \equiv$ time; $T \equiv$ temperature

*Where τ_{ij} is the force exerted in the jth direction on a unit area of fluid surface of constant x_i by fluid in the region lesser x_i on fluid in the region greater x_i [see "*Note on the Sign Convention for the Stress Tensor*" on pp. 19-20 of Bird *et al.* (2007), or pp. 24-25 of Bird *et al.* (2015)].

Table 2. Dimensionless variables and groups.

Name	Symbol	Eq.
Carreau first normal stress coefficient, infinite shear rate	$\mathbb{N}_{1\infty} \equiv \Psi_{1\infty}/\Psi_{10}$	(60)
Carreau index, first normal	n'_C	(7)
Carreau index, second normal	n''_C	(8)
Carreau index, shear	n_C	(6)
Carreau second normal stress coefficient, infinite shear rate	$\mathbb{N}_{2\infty} \equiv \Psi_{2\infty}/\Psi_{20}$	(73)
Carreau viscosity, infinite shear rate	$\mathbb{H}_\infty \equiv \eta_\infty/\eta_0$	(47)
Carreau Weissenberg number, first normal	$\mathrm{Wi}'_\mathrm{C} \equiv \lambda'_\mathrm{C}\dot{\gamma}$	(61)
Carreau Weissenberg number, first notmal, inflection	$\mathrm{Wi}'_\mathrm{Ci} \equiv \lambda'_\mathrm{C}\dot{\gamma}_\mathrm{i}$	(67)
Carreau Weissenberg number, second normal	$\mathrm{Wi}''_\mathrm{C} \equiv \lambda''_\mathrm{C}\dot{\gamma}$	(74)
Carreau Weissenberg number, second normal, inflection	$\mathrm{Wi}''_\mathrm{Ci} \equiv \lambda''_\mathrm{C}\dot{\gamma}_\mathrm{i}$	(80)
Carreau Weissenberg number, shear	$\mathrm{Wi}_\mathrm{C} \equiv \lambda_\mathrm{C}\dot{\gamma}$	(48)
Carreau Weissenberg number, shear, inflection	$\mathrm{Wi}_\mathrm{Ci} \equiv \lambda_\mathrm{C}\dot{\gamma}_\mathrm{i}$	(54)
Coefficient in Eq. (199)	Σ_R	(199)
Coefficient in Eqs. (181) and (182)	α_t	(181), (182)
Coefficient in Eq. (192)	ϕ	(192)
Coefficient in Eq. (193)	Λ_k	(193)
Coefficient in Eq. (195)	ϕ_i	(195)
Coefficient in Eq. (196)	$\Lambda_{k,\mathrm{i}}$	(196)
Exponent in Eq. (57)	δ	(58)
Exponent in Eq. (70)	δ'	(71)
Exponent in Eq. (83)	δ''	(84)
Leider number	$\mathrm{Ld} \equiv n\lambda'/t_p$	(165)
Oldroyd constant ratio	$\sigma \equiv \sigma_2/\sigma_1 = \eta_\infty/\eta_0$	(19), (20)
Oldroyd constant ratio, n-th spectrum	$\sigma_n \equiv \sigma_{2n}/\sigma_{1n}$	(94)
Power-law index, first normal	n'	(41)
Power-law index, second normal	n''	(42)
Power-law index, shear	n	(40)
Riemann zeta function	$\zeta(\alpha) \equiv \sum_{k=1}^{\infty} \frac{1}{k^\alpha}$	(184)
Weissenberg number, shear	$\mathrm{Wi} \equiv \lambda\dot{\gamma}$	
Weissenberg number, shear, inflection	$\mathrm{Wi}_\mathrm{i} \equiv \lambda\dot{\gamma}_\mathrm{i}$	

$$\Psi_1(\dot{\gamma}) = m'\dot{\gamma}^{n'-2} \tag{2}$$

$$\Psi_2(\dot{\gamma}) = -m''\dot{\gamma}^{n''-2} \tag{3}$$

each of which, thus, has a slope (n–1, n'–2 and n''–2) and an intercept (ln m, ln m' and ln m''). In the event that either $\eta(\dot{\gamma})$, $\Psi_1(\dot{\gamma})$ or $\Psi_2(\dot{\gamma})$ do not inflect, when any of these functions approach asymptotes as $\dot{\gamma}\to\infty$, we can identify the tangents given by Eqs. (1)-(3) with these asymptotes. We call these tangents *power-laws*, and the parameters n, n' and n'', *power-law indexes*, and the factors m, m' and m'', *power-law coefficients*.

With the pairing of Eqs. (1) and (2), we uncover the *first inflection pairing time* [Eq. (5.2-54) of Bird *et al.* (1977) or Eq. (4.2-68) of Bird *et al.* (1987); Eq. (2) of Leider (1974) or Eq. (20) of Leider and Bird (1974)]:

$$\lambda'_B \equiv \left(\frac{m'}{2m}\right)^{1/(n'-n)} \tag{4}$$

and with Eqs. (1) and (3), the *second inflection pairing time*:

$$\lambda''_B \equiv \left(\frac{m''}{2m}\right)^{1/(n''-n)} \tag{5}$$

which we will explore in Subsection 3.2 for the Oldroyd 8-constant model. λ'_B arises in quasi-steady state solutions to squeezing flow problems [see EXAMPLE 5.2-6 of Bird *et al.* (1977)].

Whereas log-log plots of viscosity *versus* shear rate will inflect at Wi_i, the linear-linear plot of viscosity *versus* shear rate will, of course, inflect at Weissenberg number well below Wi_i. These linear-linear inflections are not to be confused with inflections of log-log plots of viscosity *versus* shear rate. Linear-linear inflections are beyond the scope of this paper.

1.1. Carreau model

In this paper, we shall first deepen our understanding of the inflection of the viscosity curve using the *Carreau model* [see Eq. 5.1-13 in Bird *et al.* (1977)]:

$$\frac{\eta-\eta_\infty}{\eta_0-\eta_\infty} = [1+(\lambda_C\dot{\gamma})^2]^{(n_C-1)/2} \tag{6}$$

where three of the parameters have clear physical significance: η_0 is the zero-shear viscosity, η_∞ is the infinite shear rate viscosity and λ_C is the characteristic time for the Carreau fluid. By inspection, we see that n_C governs the rate of descent for the case of shear-thinning, where $\eta_0 > \eta_\infty$. Further, the lower the value of n_C, the lower the value of $\lambda_C\dot{\gamma}$ at which the viscosity approaches its lower limit, η_∞. If $n_C > 1$, Eq. (6) gives $\lim_{\dot{\gamma}\to\infty}\eta = +\infty$, which is why Eq. (6) cannot adequately describe shear-thickening. In this paper, we will derive an expression for the slope of the steady shear viscosity curve at its inflection, (n–1), to discover how n, shear power-law index, is related to the parameters in Eq. (6): η_0, η_∞, λ_C or n_C. In this connection, we observe that viscosity curves predicted by Eq. (6) are not two-fold symmetric about the inflection. Specifically, the roll-off to the straight region is always more rapid than the approach to the lower limit, η_∞.

Of course, though never done, Eq. (6) can be re-proposed easily for the first normal stress coefficient:

$$\frac{\Psi_1-\Psi_{1\infty}}{\Psi_{10}-\Psi_{1\infty}} = \left[1+\left(\lambda'_C\dot{\gamma}\right)^2\right]^{(n'_C-2)/2} \tag{7}$$

and also, for the second:

$$\frac{\Psi_2-\Psi_{2\infty}}{\Psi_{20}-\Psi_{2\infty}} = \left[1+\left(\lambda''_C\dot{\gamma}\right)^2\right]^{(n''_C-2)/2} \tag{8}$$

We will use Eqs. (6) and (7) in Subsection 3.1.

1.2. Oldroyd 8-constant model

Of course, in steady shear flow, the curves for the first normal stress coefficient, $\Psi_1(\dot{\gamma})$, and for the second normal stress coefficient, $\Psi_2(\dot{\gamma})$, also inflect. To deepen our understanding of these inflections, and of their relations to viscosity inflections, we consider the more general constitutive equation, the Oldroyd 8-constant model:

$$\boldsymbol{\tau} + \lambda_1\frac{\mathscr{D}\boldsymbol{\tau}}{\mathscr{D}t} + \tfrac{1}{2}\mu_0(\mathrm{tr}\boldsymbol{\tau})\dot{\boldsymbol{\gamma}} - \tfrac{1}{2}\mu_1\{\boldsymbol{\tau}\cdot\dot{\boldsymbol{\gamma}}+\dot{\boldsymbol{\gamma}}\cdot\boldsymbol{\tau}\} + \tfrac{1}{2}\nu_1(\boldsymbol{\tau}:\dot{\boldsymbol{\gamma}})\boldsymbol{\delta}$$
$$= -\eta_0\left(\dot{\boldsymbol{\gamma}} + \lambda_2\frac{\mathscr{D}\dot{\boldsymbol{\gamma}}}{\mathscr{D}t} - \mu_2\{\dot{\boldsymbol{\gamma}}\cdot\dot{\boldsymbol{\gamma}}\} + \tfrac{1}{2}\nu_2(\dot{\boldsymbol{\gamma}}:\dot{\boldsymbol{\gamma}})\boldsymbol{\delta}\right) \tag{9}$$

which reduces to many important models as special cases. In Eq. (9), the total stress tensor is given by:

$$\boldsymbol{\pi} \equiv \boldsymbol{\tau} + p\boldsymbol{\delta} \tag{10}$$

and the rate-of-deformation tensor, by:

$$\dot{\boldsymbol{\gamma}} \equiv \nabla\mathbf{v} + (\nabla\mathbf{v})^\dagger \tag{11}$$

and the corotational derivative, by:

$$\frac{\mathscr{D}\mathbf{b}}{\mathscr{D}t} \equiv \frac{D\mathbf{b}}{Dt} + \tfrac{1}{2}\{\boldsymbol{\omega}\cdot\boldsymbol{\tau} - \boldsymbol{\tau}\cdot\boldsymbol{\omega}\} \tag{12}$$

where the vorticity tensor is defined by:

$$\boldsymbol{\omega} \equiv \nabla\mathbf{v} - (\nabla\mathbf{v})^\dagger \tag{13}$$

In Eq. (10), δ is the *kronecker delta*. The Oldroyd 8-constant model can be remarkably useful in polymer processing when it leads to analytical solutions, as it does for wire coating [Case III in Jones (1964)], and to a corrugated wire coated through a corrugated die [see Section 3. of Jones and Jones (1966); Section 2. of Jones (1967)], and in plastic pipe extrusion for elliptical pipe [see Jones (1965); Camileri and Jones (1966)], and also to extrusion from an eccentric annular pipe die [Case II in Jones (1964); Saengow *et al.* (2015 a and b)].

For steady shear flow, Eq. (9) yields [Eq. (8) of Jones (1964)]:

$$\frac{\eta(\dot{\gamma})}{\eta_0} = \frac{1+\sigma_2\dot{\gamma}^2}{1+\sigma_1\dot{\gamma}^2} \tag{14}$$

where:

$$\sigma_1 \equiv \lambda_1^2 + \mu_0\left(\mu_1 - \tfrac{3}{2}\nu_1\right) - \mu_1\left(\mu_1 - \nu_1\right) \tag{15}$$

$$\sigma_2 \equiv \lambda_1\lambda_2 + \mu_0\left(\mu_2 - \tfrac{3}{2}\nu_2\right) - \mu_1\left(\mu_2 - \nu_2\right) \tag{16}$$

Introducing the Weissenberg number:

$$\mathrm{Wi} \equiv \sqrt{\sigma_1}\dot{\gamma} \tag{17}$$

into Eq. (14) gives:

$$\frac{\eta}{\eta_0} = \frac{1+\sigma\,\mathrm{Wi}^2}{1+\mathrm{Wi}^2} \tag{18}$$

where:

$$\sigma \equiv \sigma_2/\sigma_1 \tag{19}$$

From Eq. (17), we identify the first characteristic time of the fluid as $\lambda \equiv \sqrt{\sigma_1}$. Taking the limit as strain rate, $\dot{\gamma}$, goes to infinity yields:

$$\eta_\infty/\eta_0 = \sigma \tag{20}$$

which assigns clear physical significance to σ. The Oldroyd 8-constant model thus predicts viscosity curve shapes with just three parameters: σ_1, η_0 and σ (one less than the Carreau model). From Eq. (18) we learn that, for the shear stress to increase monotonically with shear rate, we need:

$$\sigma \geq 1/9 \tag{21}$$

From Eq. (18), we see that σ governs the rate of descent for the case of shear-thinning, where $\eta_0 > \eta_\infty$, and the rate of ascent where $\eta_0 < \eta_\infty$. Thus, Eq. (18) is as useful for describing shear-thickening ($\sigma > 1$) as it is for shear-thinning ($\sigma < 1$) [see Fig. 1]. Whereas, for the Carreau model, the viscosity begins its descent toward the straight region at $\lambda\dot{\gamma} \approx 1$, for the Oldroyd 8-constant model, these approaches begin at $\lambda\dot{\gamma} \approx 1/10$ (for all values of σ). Further, the viscosity approaches its limit, η_∞, at $\lambda\dot{\gamma} \approx 10$ (for all values of σ). In this paper, we will derive an expression for the slope of the steady shear viscosity curve at its inflection, $(n-1)$, to discover how n is related to the parameters in Eq. (18): σ_1, η_0 or σ. In this connection, we observe that viscosity curves predicted by Eq. (18) are not two-fold symmetric about the inflection. Specifically, the approach to the straight region is always more rapid than the approach to the limit, η_∞ (for all values of σ).

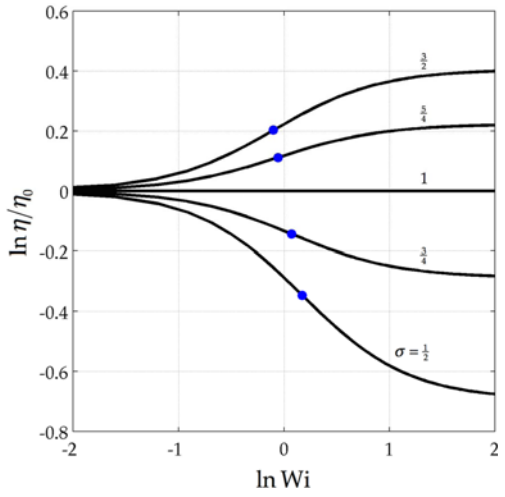

Fig. 1. Dimensionless viscosity curves for shear thinning ($\sigma = \frac{1}{2}, \frac{3}{4}$), Newtonian ($\sigma = 1$) and shear thickening ($\sigma = \frac{5}{4}, \frac{3}{2}$) behaviors. Blue dots indicate inflections given by Eq. (90) [Oldroyd 8-constant].

For the normal stress difference coefficients, for the Oldroyd 8-constant model, in steady shear flow, we get [Eq. (12) of Oldroyd (1958)]:

$$\frac{\Psi_1(\dot{\gamma})}{\Psi_{10}} = \frac{\frac{\lambda_2}{\lambda_1} - \frac{\eta(\dot{\gamma})}{\eta_0}}{\frac{\lambda_2}{\lambda_1} - 1} \tag{22}$$

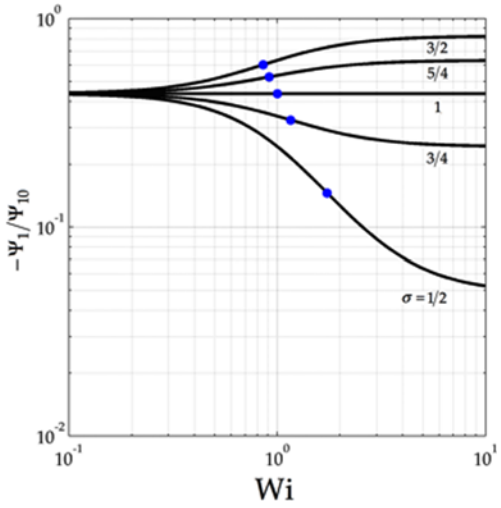

Fig. 2. Dimensionless first normal stress difference coefficient curves for shear thinning ($\sigma = \frac{1}{2}, \frac{3}{4}$), Newtonian ($\sigma = 1$) and shear thickening ($\sigma = \frac{5}{4}, \frac{3}{2}$) behaviors [Eq. (22)], for every curve, $\lambda_1 = 10$s and $\lambda_2 = 4$s. Blue dots indicate inflections given by Eq. (118) [Oldroyd 8-constant].

and:

$$\frac{\Psi_2(\dot{\gamma})}{\Psi_{20}} = \frac{(\lambda_1 - \mu_1)}{(\lambda_1 - \lambda_2 - \mu_1 + \mu_2)}\frac{\eta(\dot{\gamma})}{\eta_0} - \frac{(\lambda_2 - \mu_2)}{(\lambda_1 - \lambda_2 - \mu_1 + \mu_2)} \tag{23}$$

where $\eta(\dot{\gamma})/\eta_0$ is given by Eq. (14), and where:

$$\Psi_{10} = 2\eta_0\left(\lambda_1 - \lambda_2\right) \tag{24}$$

and:

$$\Psi_{20} = -\eta_0\left(\lambda_1 - \lambda_2 - \mu_1 + \mu_2\right) \tag{25}$$

Hence:

$$\frac{-\Psi_2(\dot{\gamma})}{\Psi_1(\dot{\gamma})} = \frac{1}{2}\left[\frac{\lambda_1 - \mu_1}{\lambda_1 - \lambda_2\dfrac{\eta(\dot{\gamma})}{\eta_0}} - \frac{\lambda_2 - \mu_2}{\lambda_1\dfrac{\eta(\dot{\gamma})}{\eta_0} - \lambda_2}\right] \tag{26}$$

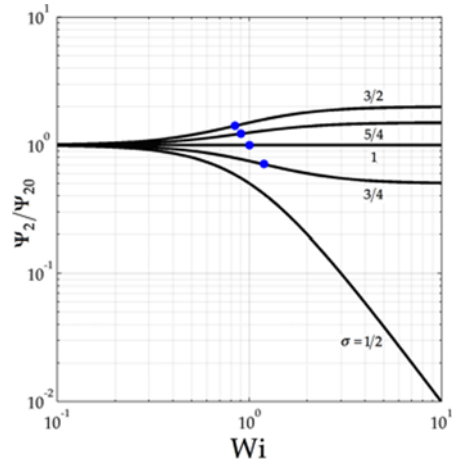

Fig. 3. Dimensionless first normal stress difference coefficient curves for shear thinning ($\sigma = \frac{1}{2}, \frac{3}{4}$), Newtonian ($\sigma = 1$) and shear thickening ($\sigma = \frac{5}{4}, \frac{3}{2}$) behaviors [Eq. (23) with Eq. (18)], for every curve, $\lambda_1 = 10$s and $\lambda_2 = 4$s. Blue dots indicate inflections given by Eq. (144) [with Eqs. (139) and (140)]. The lowest curve does not inflect [Oldroyd 8-constant].

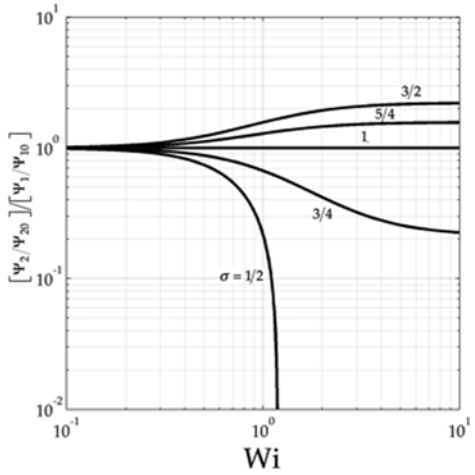

Fig. 4. Ratio of second to first normal stress difference coefficient curves for shear thinning ($\sigma = \frac{1}{2}, \frac{3}{4}$), Newtonian ($\sigma = 1$) and shear thickening ($\sigma = \frac{5}{4}, \frac{3}{2}$) behaviors [Eq. (26) with Eqs. (24) and (25)] [Oldroyd 8-constant].

Substituting Eq. (18) into Eq. (22) then taking the limit as $\lambda\dot{\gamma} \to \infty$ of Eqs. (22) and (23) gives:

$$\frac{\Psi_{1\infty}}{\Psi_{10}} \equiv \lim_{\lambda\dot{\gamma}\to\infty} \frac{\Psi_1(\dot{\gamma})}{\Psi_{10}} = \frac{\lambda_2 - \lambda_1\sigma}{\lambda_2 - \lambda_1} \tag{27}$$

and

$$\frac{\Psi_{2\infty}}{\Psi_{10}} \equiv \lim_{\lambda\dot{\gamma}\to\infty} \frac{\Psi_2(\dot{\gamma})}{\Psi_{20}} = \frac{(\lambda_1 - \mu_1)\sigma - (\lambda_2 - \mu_2)}{(\lambda_1 - \mu_1) - (\lambda_2 - \mu_2)} \tag{28}$$

the ordinates of the first and second normal stress coefficients. We will use Eqs. (14), (22) and (23) to evaluate our inflections below.

In Section 5, we provide worked examples for both the Carreau (Subsection 5.1) and the Oldroyd 8-constant models (Subsection 5.2). These examples illustrate how to calculate the inflections in all three viscometric functions, $\eta(\dot{\gamma})$, $\Psi_1(\dot{\gamma})$ and $\Psi_2(\dot{\gamma})$.

2. Differentiating Viscometric Fuctions

In this section, we prepare the expressions that we will use to find inflections. Since:

$$d\ln\eta = \frac{1}{\eta}d\eta \tag{29}$$

and:

$$d\ln\dot{\gamma} = \frac{1}{\dot{\gamma}}d\dot{\gamma} \tag{30}$$

for the viscosity curve slope, we get:

$$\frac{d\ln\eta}{d\ln\dot{\gamma}} = \frac{\dot{\gamma}}{\eta}\frac{d\eta}{d\dot{\gamma}} \tag{31}$$

which is why the slope of a viscosity curve is always dimensionless. We can also nondimensionalize the variables in Eq. (31) as:

$$\frac{d\ln(\eta/\eta_0)}{d\ln(\lambda\dot{\gamma})} = \frac{d\ln\eta}{d\ln\dot{\gamma}} = \frac{\lambda\dot{\gamma}}{\eta/\eta_0}\frac{d(\eta/\eta_0)}{d(\lambda\dot{\gamma})} \tag{32}$$

For the second derivative of a viscosity curve we have:

$$\frac{d^2\ln\eta}{d(\ln\dot{\gamma})^2} = \frac{d}{d\ln\dot{\gamma}}\left(\frac{\dot{\gamma}}{\eta}\frac{d\eta}{d\dot{\gamma}}\right) \tag{33}$$

and again using Eq. (30):

$$\frac{d^2\ln\eta}{d(\ln\dot{\gamma})^2} = \dot{\gamma}\frac{d}{d\dot{\gamma}}\left(\frac{\dot{\gamma}}{\eta}\frac{d\eta}{d\dot{\gamma}}\right) = \frac{\dot{\gamma}}{\eta^2}\left(\eta - \dot{\gamma}\frac{d\eta}{d\dot{\gamma}}\right)\frac{d\eta}{d\dot{\gamma}} + \frac{\dot{\gamma}^2}{\eta}\frac{d^2\eta}{d\dot{\gamma}^2} \tag{34}$$

which is thus also dimensionless, and whose variables can also be nondimensionalized as:

$$\frac{d^2\ln(\eta/\eta_0)}{d(\ln\lambda\dot{\gamma})^2} = \frac{d^2\ln\eta}{d(\ln\dot{\gamma})^2} = \frac{\lambda\dot{\gamma}}{(\eta/\eta_0)^2}\left[(\eta/\eta_0) - \lambda\dot{\gamma}\frac{d(\eta/\eta_0)}{d(\lambda\dot{\gamma})}\right]\frac{d(\eta/\eta_0)}{d(\lambda\dot{\gamma})} + \frac{(\lambda\dot{\gamma})^2}{\eta/\eta_0}\frac{d^2(\eta/\eta_0)}{d(\lambda\dot{\gamma})^2} \tag{35}$$

which we will use in the next Section to find inflections. Whereas locating the end of the Newtonian plateau of a viscosity curve is somewhat arbitrary, locating its inflection point is less so.

Similarly, for the first normal stress coefficient, replacing η with Ψ_1 and η_0 with Ψ_{10} in Eqs. (32) and (35) gives:

$$\frac{d\ln(\Psi_1/\Psi_{10})}{d\ln(\lambda\dot{\gamma})} = \frac{d\ln\Psi_1}{d\ln\dot{\gamma}} = \frac{\lambda\dot{\gamma}}{\Psi_1/\Psi_{10}}\frac{d(\Psi_1/\Psi_{10})}{d(\lambda\dot{\gamma})} \tag{36}$$

$$\frac{d^2\ln(\Psi_1/\Psi_{10})}{d(\ln\lambda\dot{\gamma})^2} = \frac{\lambda\dot{\gamma}}{(\Psi_1/\Psi_{10})^2}\left[(\Psi_1/\Psi_{10}) - \lambda\dot{\gamma}\frac{d(\Psi_1/\Psi_{10})}{d(\lambda\dot{\gamma})}\right]\frac{d(\Psi_1/\Psi_{10})}{d(\lambda\dot{\gamma})} + \frac{(\lambda\dot{\gamma})^2}{\Psi_1/\Psi_{10}}\frac{d^2(\Psi_1/\Psi_{10})}{d(\lambda\dot{\gamma})^2} \tag{37}$$

and, for the second normal stress coefficient, we get:

$$\frac{d\ln(\Psi_2/\Psi_{20})}{d\ln(\lambda\dot{\gamma})}=\frac{\lambda\dot{\gamma}}{\Psi_2/\Psi_{20}}\frac{d(\Psi_2/\Psi_{20})}{d(\lambda\dot{\gamma})} \tag{38}$$

$$\frac{d^2\ln(\Psi_2/\Psi_{20})}{d(\ln\lambda\dot{\gamma})^2}=\frac{\lambda\dot{\gamma}}{(\Psi_2/\Psi_{20})^2}\left[(\Psi_2/\Psi_{20})-\lambda\dot{\gamma}\frac{d(\Psi_2/\Psi_{20})}{d(\lambda\dot{\gamma})}\right]\frac{d(\Psi_2/\Psi_{20})}{d(\lambda\dot{\gamma})}+\frac{(\lambda\dot{\gamma})^2}{\Psi_2/\Psi_{20}}\frac{d^2(\Psi_2/\Psi_{20})}{d(\lambda\dot{\gamma})^2} \tag{39}$$

We will use Eqs. (32) and (35)-(39) to find the inflection tangents, for the viscosity curve [Eq. (1)] for the first normal stress coefficient curve [Eq. (2)] and for the second normal stress coefficient [Eq. (3)] in steady shear flow.

3. Finding Inflections

We define the slope of the tangent where the viscosity curve inflects as $(n-1)$, where n is called the *shear power-law index*:

$$(n-1)\equiv\left.\frac{d\ln(\eta/\eta_0)}{d\ln(\lambda\dot{\gamma})}\right|_{\mathrm{Wi_i}}=\left.\frac{d\ln\eta}{d\ln\dot{\gamma}}\right|_{\mathrm{Wi_i}} \tag{40}$$

where the first normal stress coefficient curve inflects as $(n'-2)$, where n' is called the *first normal power-law index*:

$$(n'-2)\equiv\left.\frac{d\ln(\Psi_1/\Psi_{10})}{d\ln(\lambda\dot{\gamma})}\right|_{\mathrm{Wi_i}}=\left.\frac{d\ln\Psi_1}{d\ln\dot{\gamma}}\right|_{\mathrm{Wi_i}} \tag{41}$$

and where the second normal stress coefficient curve inflects as $(n''-2)$, where n'' is called the *second normal power-law index*:

$$(n''-2)\equiv\left.\frac{d\ln(\Psi_2/\Psi_{20})}{d\ln(\lambda\dot{\gamma})}\right|_{\mathrm{Wi_i}}=\left.\frac{d\ln\Psi_2}{d\ln\dot{\gamma}}\right|_{\mathrm{Wi_i}} \tag{42}$$

With each of these inflection tangents, through Eqs. (1)-(3), we associate a dimensional coefficient:

$$m=\frac{\eta_{\mathrm{i}}}{\dot{\gamma}_{\mathrm{i}}^{\,n-1}} \tag{43}$$

$$m'=\frac{\Psi_{1\mathrm{i}}}{\dot{\gamma}_{\mathrm{i}}^{\,n'-2}} \tag{44}$$

$$m''=\frac{-\Psi_{2\mathrm{i}}}{\dot{\gamma}_{\mathrm{i}}^{\,n''-2}} \tag{45}$$

where $(\eta_{\mathrm{i}},\dot{\gamma}_{\mathrm{i}})$, $(\Psi_{1\mathrm{i}},\dot{\gamma}_{\mathrm{i}})$ and $(\Psi_{2\mathrm{i}},\dot{\gamma}_{\mathrm{i}})$ are the inflection points. Mindful of Table 1, we see that the single prime and double prime denote the quantities associated with the first and second normal stress differences. We will need Eqs. (40)-(45) to evaluate λ_{B}' and λ_{B}'' for the Oldroyd 8-constant model in Subsection 3.2.

3.1. Carreau model

For the steady shear viscosity, we first calculate the inflection tangent slope for the Carreau model defined in Eq. (6) which we rewrite as:

$$\frac{\eta}{\eta_0}=(1-\mathbb{H}_\infty)\left[1+\mathrm{Wi_C^2}\right]^{(n_{\mathrm{C}}-1)/2}+\mathbb{H}_\infty \tag{46}$$

where we call n_{C} the *shear Carreau index*, and where:

$$\mathbb{H}_\infty\equiv\frac{\eta_\infty}{\eta_0} \tag{47}$$

is the *dimensionless infinite shear rate viscosity*, and where the *shear Carreau Weissenberg number* is given by:

$$\mathrm{Wi_C}\equiv\lambda_{\mathrm{C}}\dot{\gamma} \tag{48}$$

where λ_{C} is the *shear Carreau characteristic time*.

For the special case of $\eta_\infty=0$, we see that Eq. (46) approaches:

$$\frac{\eta}{\eta_0}=\left[1+\mathrm{Wi_C^2}\right]^{(n_{\mathrm{C}}-1)/2} \tag{49}$$

asymptotically. Eq. (46) intercepts the ordinate at:

$$\frac{\eta}{\eta_0}=1 \tag{50}$$

as it must. We can thus only identify the shear Carreau index, n_{C}, with the shear power-law index, n, for the special case of $\eta_\infty=0$ [see after Eq. (57)].

Differentiating Eq. (46) once gives:

$$\frac{d(\eta/\eta_0)}{d\,\mathrm{Wi_C}}=(1-\mathbb{H}_\infty)(n_{\mathrm{C}}-1)\,\mathrm{Wi_C}\left(1+\mathrm{Wi_C^2}\right)^{\frac{n_{\mathrm{C}}-3}{2}} \tag{51}$$

or twice:

$$\frac{d^2(\eta/\eta_0)}{d\,\mathrm{Wi_C^2}}=(1-\mathbb{H}_\infty)(n_{\mathrm{C}}-1)\times\left[(n_{\mathrm{C}}-3)\,\mathrm{Wi_C^2}\left(1+\mathrm{Wi_C^2}\right)^{\frac{n_{\mathrm{C}}-5}{2}}+\left(1+\mathrm{Wi_C^2}\right)^{\frac{n_{\mathrm{C}}-3}{2}}\right] \tag{52}$$

Substituting Eqs. (46), (51) and (52) into Eq. (35) then simplifying gives:

$$\frac{d^2\ln(\eta/\eta_0)}{d(\ln\mathrm{Wi_C})^2}=\frac{(1-\mathbb{H}_\infty)(n_{\mathrm{C}}-1)\,\mathrm{Wi_C^2}}{\left[(1-\mathbb{H}_\infty)\left(1+\mathrm{Wi_C^2}\right)^{\frac{n_{\mathrm{C}}-1}{2}}+\mathbb{H}_\infty\right]^2}\times\left[\begin{array}{l}2(1-\mathbb{H}_\infty)\left(1-\dfrac{\mathrm{Wi_C^2}}{1+\mathrm{Wi_C^2}}\right)\left(1+\mathrm{Wi_C^2}\right)^{n_{\mathrm{C}}-2}\\+\mathbb{H}_\infty\left(2+\dfrac{(n-3)\,\mathrm{Wi_C^2}}{1+\mathrm{Wi_C^2}}\right)\left(1+\mathrm{Wi_C^2}\right)^{\frac{n_{\mathrm{C}}-3}{2}}\end{array}\right] \tag{53}$$

Setting Eq. (53) to zero gives the transcendental function for the *shear Carreau inflection Weissenberg number*, $\mathrm{Wi_{Ci}}\equiv\lambda_{\mathrm{C}}\dot{\gamma}_{\mathrm{i}}$:

$$0=\frac{(1-\mathbb{H}_\infty)(n_{\mathrm{C}}-1)\,\mathrm{Wi_{Ci}^2}}{\left[(1-\mathbb{H}_\infty)\left(1+\mathrm{Wi_{Ci}^2}\right)^{\frac{n_{\mathrm{C}}-1}{2}}+\mathbb{H}_\infty\right]^2}\times\left[\begin{array}{l}2(1-\mathbb{H}_\infty)\left(1-\dfrac{\mathrm{Wi_{Ci}^2}}{1+\mathrm{Wi_{Ci}^2}}\right)\left(1+\mathrm{Wi_{Ci}^2}\right)^{n_{\mathrm{C}}-2}\\+\mathbb{H}_\infty\left(2+\dfrac{(n_{\mathrm{C}}-3)\,\mathrm{Wi_{Ci}^2}}{1+\mathrm{Wi_{Ci}^2}}\right)\left(1+\mathrm{Wi_{Ci}^2}\right)^{\frac{n_{\mathrm{C}}-3}{2}}\end{array}\right] \tag{54}$$

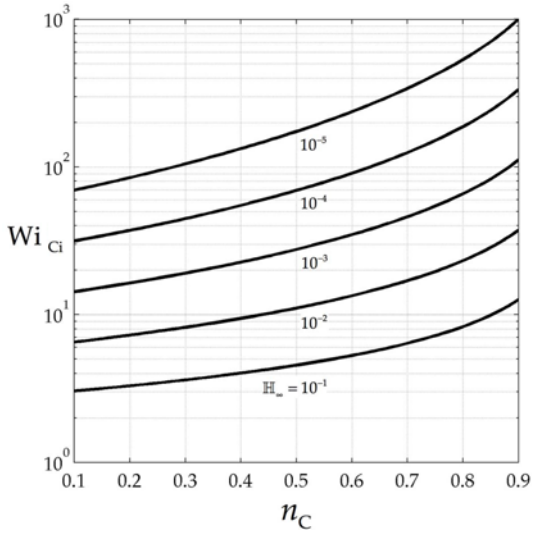

Fig. 5. Weissenberg number at inflection point *versus* shear Carreau index (n_{C}) with curves of constant $\mathbb{H}_\infty$=10^{-1}, 10^{-2}, 10^{-3}, 10^{-4}, 10^{-5} [Eq. (54)].

which is implicit in $\mathrm{Wi}_{\mathrm{Ci}}$. Fig. 5 plots $\mathrm{Wi}_{\mathrm{Ci}}$ *versus* n_{C} parametrized with $\mathbb{H}_\infty$. It can thus be used to find $\mathrm{Wi}_{\mathrm{Ci}}$ graphically, and this can then be inserted into:

$$\frac{\eta_{\mathrm{i}}}{\eta_0} = \left(1-\mathbb{H}_\infty\right)\left[1+\mathrm{Wi}_{\mathrm{Ci}}^2\right]^{(n_{\mathrm{C}}-1)/2} + \mathbb{H}_\infty \tag{55}$$

to get the ordinate value of the inflection, $\ln\eta_{\mathrm{i}}$, on the steady shear viscosity curve. Substituting Eqs. (46) and (51) into Eq. (32), then evaluating at $\mathrm{Wi}_{\mathrm{C}} = \mathrm{Wi}_{\mathrm{Ci}}$, gives the tangent inflection slope defined by Eq. (40):

$$(n-1) = \frac{(n_{\mathrm{C}}-1)\,\mathrm{Wi}_{\mathrm{Ci}}^2\left[1+\mathrm{Wi}_{\mathrm{Ci}}^2\right]^{(n_{\mathrm{C}}-3)/2}}{\left[1+\mathrm{Wi}_{\mathrm{Ci}}^2\right]^{(n_{\mathrm{C}}-1)/2} + \mathbb{H}_\infty/\left(1-\mathbb{H}_\infty\right)} \tag{56}$$

then substituting the result into Eq. (43) [with $\dot\gamma = \mathrm{Wi}_{\mathrm{Ci}}/\lambda_{\mathrm{C}}$] gives:

$$m = \eta_{\mathrm{i}}\left(\frac{\mathrm{Wi}_{\mathrm{Ci}}}{\lambda_{\mathrm{C}}}\right)^{\delta} \tag{57}$$

where:

$$\delta \equiv \frac{(1-n_{\mathrm{C}})\,\mathrm{Wi}_{\mathrm{Ci}}^2\left[1+\mathrm{Wi}_{\mathrm{Ci}}^2\right]^{(n_{\mathrm{C}}-3)/2}}{\left[1+\mathrm{Wi}_{\mathrm{Ci}}^2\right]^{(n_{\mathrm{C}}-1)/2} + \mathbb{H}_\infty/\left(1-\mathbb{H}_\infty\right)} \tag{58}$$

Eq. (56) shows why, in general, where $\eta_\infty > 0$, n differs from n_{C}, and thus cannot be identified with n_{C}.

Next, for the first normal stress coefficient, we calculate the inflection tangent slope for the Carreau model defined in Eq. (7) which we rewrite as:

$$\frac{\Psi_1}{\Psi_{10}} = \left(1-\mathbb{N}_{1\infty}\right)\left[1+\mathrm{Wi}_{\mathrm{C}}'^2\right]^{\frac{n_{\mathrm{C}}'-1}{2}} + \mathbb{N}_{1\infty} \tag{59}$$

where we call n_{C}' the *first normal Carreau index*, and where:

$$\mathbb{N}_{1\infty} \equiv \frac{\Psi_{1\infty}}{\Psi_{10}} \tag{60}$$

is the *dimensionless infinite shear rate Carreau first normal stress coefficient*, and where the *first normal Carreau Weissenberg number* is defined by:

$$\mathrm{Wi}_{\mathrm{C}}' \equiv \lambda_{\mathrm{C}}'\dot\gamma \tag{61}$$

where λ_{C} is the *first normal Carreau relaxation time*.

For the special case of $\Psi_{1\infty} = 0$, we see that Eq. (59) approaches:

$$\frac{\Psi_1}{\Psi_{10}} = \left[1+\mathrm{Wi}_{\mathrm{C}}'^2\right]^{\frac{n_{\mathrm{C}}'-1}{2}} \tag{62}$$

asymptotically. Eq. (59) intercepts the ordinate at:

$$\frac{\Psi_1}{\Psi_{10}} = 1 \tag{63}$$

as it must. We can thus identify the first normal Carreau index, n_{C}', with the first normal power-law index, n', for the special case of $\Psi_{1\infty} = 0$.

Differentiating Eq. (59) once gives:

$$\frac{d\left(\Psi_1/\Psi_{10}\right)}{d\,\mathrm{Wi}_{\mathrm{C}}'} = \left(1-\mathbb{N}_{1\infty}\right)\left(n_{\mathrm{C}}'-2\right)\mathrm{Wi}_{\mathrm{C}}'\left(1+\mathrm{Wi}_{\mathrm{C}}'^2\right)^{\frac{n_{\mathrm{C}}'}{2}-2} \tag{64}$$

or twice:

$$\frac{d^2\left(\Psi_1/\Psi_{10}\right)}{d\,\mathrm{Wi}_{\mathrm{C}}'^2} = \left(1-\mathbb{N}_{1\infty}\right)\left(n_{\mathrm{C}}'-2\right) \times\left[\left(n_{\mathrm{C}}'-4\right)\mathrm{Wi}_{\mathrm{C}}'^2\left(1+\mathrm{Wi}_{\mathrm{C}}'^2\right)^{\frac{n_{\mathrm{C}}'}{2}-3} + \left(1+\mathrm{Wi}_{\mathrm{C}}'^2\right)^{\frac{n_{\mathrm{C}}'}{2}-2}\right] \tag{65}$$

Substituting Eqs. (59), (64) and (65) into Eq. (37) then simplifying gives:

$$\frac{d^2\ln\left(\frac{\Psi_1}{\Psi_{10}}\right)}{d\left(\ln\mathrm{Wi}_{\mathrm{C}}'\right)^2} = \frac{\left(1-\mathbb{N}_{1\infty}\right)\left(n_{\mathrm{C}}'-2\right)\mathrm{Wi}_{\mathrm{C}}'^2}{\left[\left(1-\mathbb{N}_{1\infty}\right)\left(1+\mathrm{Wi}_{\mathrm{C}}'^2\right)^{\frac{n_{\mathrm{C}}'}{2}-1} + \mathbb{N}_{1\infty}\right]^2} \times\left[\begin{array}{l} 2\left(1-\mathbb{N}_{1\infty}\right)\left(1-\dfrac{\mathrm{Wi}_{\mathrm{C}}'^2}{1+\mathrm{Wi}_{\mathrm{C}}'^2}\right)\left(1+\mathrm{Wi}_{\mathrm{C}}'^2\right)^{n_{\mathrm{C}}'-3} \\ +\mathbb{N}_{1\infty}\left(2+\dfrac{\left(n_{\mathrm{C}}'-4\right)\mathrm{Wi}_{\mathrm{C}}'^2}{1+\mathrm{Wi}_{\mathrm{C}}'^2}\right)\left(1+\mathrm{Wi}_{\mathrm{C}}'^2\right)^{\frac{n_{\mathrm{C}}'}{2}-2} \end{array}\right] \tag{66}$$

Setting this to zero gives the transcendental function for the *first normal Carreau inflection Weissenberg number*, $\mathrm{Wi}_{\mathrm{Ci}}' \equiv \lambda_{\mathrm{C}}'\dot\gamma_{\mathrm{i}}$:

$$0 = \frac{\left(1-\mathbb{N}_{1\infty}\right)\left(n_{\mathrm{C}}'-2\right)\mathrm{Wi}_{\mathrm{Ci}}'^2}{\left[\left(1-\mathbb{N}_{1\infty}\right)\left(1+\mathrm{Wi}_{\mathrm{Ci}}'^2\right)^{\frac{n_{\mathrm{C}}'}{2}-1} + \mathbb{N}_{1\infty}\right]^2} \times\left[\begin{array}{l} 2\left(1-\mathbb{N}_{1\infty}\right)\left(1-\dfrac{\mathrm{Wi}_{\mathrm{Ci}}'^2}{1+\mathrm{Wi}_{\mathrm{Ci}}'^2}\right)\left(1+\mathrm{Wi}_{\mathrm{Ci}}'^2\right)^{n_{\mathrm{C}}'-3} \\ +\mathbb{N}_{1\infty}\left(2+\dfrac{\left(n_{\mathrm{C}}'-4\right)\mathrm{Wi}_{\mathrm{Ci}}'^2}{1+\mathrm{Wi}_{\mathrm{Ci}}'^2}\right)\left(1+\mathrm{Wi}_{\mathrm{Ci}}'^2\right)^{\frac{n_{\mathrm{C}}'}{2}-2} \end{array}\right] \tag{67}$$

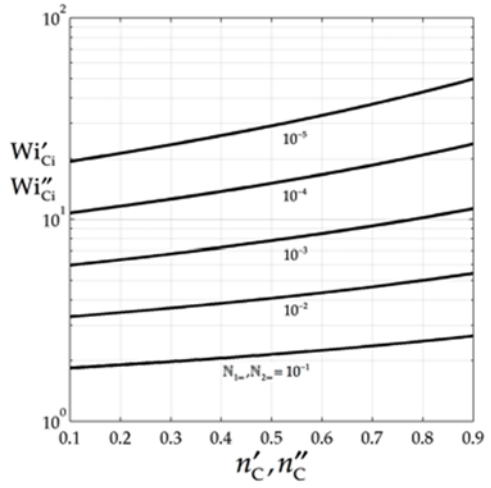

Fig. 6. Weissenberg number at inflection point *versus* first (n'_{C}) and second (n''_{C}) normal Carreau index with curves of constant $\mathbb{N}_{1\infty}=\mathbb{N}_{2\infty}$=$10^{-1}$, 10^{-2}, 10^{-3}, 10^{-4}, 10^{-5} [Eqs. (67) and (80)].

which is implicit in $\mathrm{Wi}'_{\mathrm{Ci}}$. Fig. 6 plots $\mathrm{Wi}'_{\mathrm{Ci}}$ *versus* n'_{C} parametrized with $\mathbb{N}_{1\infty}$. It can thus be used to find $\mathrm{Wi}'_{\mathrm{Ci}}$ graphically, and this can then be inserted into:

$$\frac{\Psi_{1\mathrm{i}}}{\Psi_{10}}=\left(1-\mathbb{N}_{1\infty}\right)\left[1+\mathrm{Wi}'^{2}_{\mathrm{C}}\right]^{\frac{n'_{\mathrm{C}}-1}{2}}+\mathbb{N}_{1\infty} \tag{68}$$

to get the ordinate value of the inflection, $\ln\Psi_{1\mathrm{i}}$, on the first normal stress coefficient curve. Substituting Eqs. (59) and (64) into Eq. (36) then evaluating at $\mathrm{Wi}'_{\mathrm{C}}=\mathrm{Wi}'_{\mathrm{Ci}}$ gives the tangent slope defined by Eq. (41):

$$\left(n'-2\right)=\mathrm{Wi}'_{\mathrm{Ci}}\frac{\left(1-\mathbb{N}_{1\infty}\right)\left(n'_{\mathrm{C}}-2\right)\mathrm{Wi}'_{\mathrm{Ci}}\left(1+\mathrm{Wi}'^{2}_{\mathrm{Ci}}\right)^{\frac{n'_{\mathrm{C}}-2}{2}}}{\left(1-\mathbb{N}_{1\infty}\right)\left[1+\mathrm{Wi}'^{2}_{\mathrm{Ci}}\right]^{\frac{n'_{\mathrm{C}}-1}{2}}+\mathbb{N}_{1\infty}} \tag{69}$$

then substituting the result into Eq. (44) [with $\dot{\gamma}=\mathrm{Wi}'_{\mathrm{Ci}}/\lambda'_{\mathrm{C}}$] gives:

$$m'=\Psi_{1\mathrm{i}}\left(\frac{\mathrm{Wi}'_{\mathrm{Ci}}}{\lambda_{\mathrm{C}}}\right)^{\delta'} \tag{70}$$

where:

$$\delta'\equiv\frac{\left(2-n'_{\mathrm{C}}\right)\mathrm{Wi}'^{2}_{\mathrm{Ci}}\left(1+\mathrm{Wi}'^{2}_{\mathrm{Ci}}\right)^{\left(n'_{\mathrm{C}}-4\right)/2}}{\left[1+\mathrm{Wi}'^{2}_{\mathrm{Ci}}\right]^{\left(n'_{\mathrm{C}}-2\right)/2}+\mathbb{N}_{1\infty}/\left(1-\mathbb{N}_{1\infty}\right)} \tag{71}$$

Lastly, for the second normal stress coefficient, we calculate the inflection tangent slope for the Carreau model defined in Eq. (8) which we rewrite as:

$$\frac{\Psi_2}{\Psi_{20}}=\left(1-\mathbb{N}_{2\infty}\right)\left[1+\mathrm{Wi}''^{2}_{\mathrm{C}}\right]^{\frac{n''_{\mathrm{C}}-1}{2}}+\mathbb{N}_{2\infty} \tag{72}$$

where we call n''_{C} the *second normal Carreau index*, and where:

$$\mathbb{N}_{2\infty}\equiv\frac{\Psi_{2\infty}}{\Psi_{20}} \tag{73}$$

is the *dimensionless infinite shear rate Carreau second normal stress coefficient*, and where the *second normal Carreau Weissenberg number* is defined by:

$$\mathrm{Wi}''_{\mathrm{C}}\equiv\lambda''_{\mathrm{C}}\dot{\gamma} \tag{74}$$

where λ''_{C} is the *second normal Carreau relaxation time*.

For the special case of $\Psi_{2\infty}=0$, we see that Eq. (72) approaches:

$$\frac{\Psi_2}{\Psi_{20}}=\left[1+\mathrm{Wi}''^{2}_{\mathrm{C}}\right]^{\frac{n''_{\mathrm{C}}-1}{2}} \tag{75}$$

asymptotically. Eq. (72) intercepts the ordinate at:

$$\frac{\Psi_2}{\Psi_{20}}=1 \tag{76}$$

as it must. We can thus identify the second normal Carreau index, n''_{C}, with the second normal power-law index, n'', for the special case of $\Psi_{2\infty}=0$.

Differentiating Eq. (72) once gives:

$$\frac{d\left(\Psi_2/\Psi_{20}\right)}{d\,\mathrm{Wi}''_{\mathrm{C}}}=\left(1-\mathbb{N}_{2\infty}\right)\left(n''_{\mathrm{C}}-2\right)\mathrm{Wi}''_{\mathrm{C}}\left(1+\mathrm{Wi}''^{2}_{\mathrm{C}}\right)^{\frac{n''_{\mathrm{C}}}{2}-2} \tag{77}$$

or twice:

$$\frac{d^2\left(\Psi_2/\Psi_{20}\right)}{d\,\mathrm{Wi}''^{2}_{\mathrm{C}}}=\left(1-\mathbb{N}_{2\infty}\right)\left(n''_{\mathrm{C}}-2\right)\times\left[\left(n''_{\mathrm{C}}-4\right)\mathrm{Wi}''^{2}_{\mathrm{C}}\left(1+\mathrm{Wi}''^{2}_{\mathrm{C}}\right)^{\frac{n''_{\mathrm{C}}}{2}-3}+\left(1+\mathrm{Wi}''^{2}_{\mathrm{C}}\right)^{\frac{n''_{\mathrm{C}}}{2}-2}\right] \tag{78}$$

Substituting Eqs. (72), (77) and (78) into Eq. (39) then simplifying gives:

$$\frac{d^2\ln\left(\frac{\Psi_2}{\Psi_{20}}\right)}{d\left(\ln\mathrm{Wi}''_{\mathrm{C}}\right)^2}=\frac{\left(1-\mathbb{N}_{2\infty}\right)\left(n''_{\mathrm{C}}-2\right)\mathrm{Wi}''^{2}_{\mathrm{C}}}{\left[\left(1-\mathbb{N}_{2\infty}\right)\left(1+\mathrm{Wi}''^{2}_{\mathrm{C}}\right)^{\frac{n''_{\mathrm{C}}}{2}-1}+\mathbb{N}_{2\infty}\right]^2}\times\left[\begin{array}{l}2\left(1-\mathbb{N}_{2\infty}\right)\left(1-\dfrac{\mathrm{Wi}''^{2}_{\mathrm{C}}}{1+\mathrm{Wi}''^{2}_{\mathrm{C}}}\right)\left(1+\mathrm{Wi}''^{2}_{\mathrm{C}}\right)^{n''_{\mathrm{C}}-3}\\+\mathbb{N}_{2\infty}\left(2+\dfrac{\left(n''_{\mathrm{C}}-4\right)\mathrm{Wi}''^{2}_{\mathrm{C}}}{1+\mathrm{Wi}''^{2}_{\mathrm{C}}}\right)\left(1+\mathrm{Wi}''^{2}_{\mathrm{C}}\right)^{\frac{n''_{\mathrm{C}}}{2}-2}\end{array}\right] \tag{79}$$

Setting Eq. (79) to zero gives the transcendental function for the *second normal Carreau inflection Weissenberg number*, $\mathrm{Wi}''_{\mathrm{Ci}}\equiv\lambda''_{\mathrm{C}}\dot{\gamma}_{\mathrm{i}}$:

$$0=\frac{\left(1-\mathbb{N}_{2\infty}\right)\left(n''_{\mathrm{C}}-2\right)\mathrm{Wi}''^{2}_{\mathrm{Ci}}}{\left[\left(1-\mathbb{N}_{2\infty}\right)\left(1+\mathrm{Wi}''^{2}_{\mathrm{Ci}}\right)^{\frac{n''_{\mathrm{C}}}{2}-1}+\mathbb{N}_{2\infty}\right]^2}\times\left[\begin{array}{l}2\left(1-\mathbb{N}_{2\infty}\right)\left(1-\dfrac{\mathrm{Wi}''^{2}_{\mathrm{Ci}}}{1+\mathrm{Wi}''^{2}_{\mathrm{Ci}}}\right)\left(1+\mathrm{Wi}''^{2}_{\mathrm{Ci}}\right)^{n''_{\mathrm{C}}-3}\\+\mathbb{N}_{2\infty}\left(2+\dfrac{\left(n''_{\mathrm{C}}-4\right)\mathrm{Wi}''^{2}_{\mathrm{Ci}}}{1+\mathrm{Wi}''^{2}_{\mathrm{Ci}}}\right)\left(1+\mathrm{Wi}''^{2}_{\mathrm{Ci}}\right)^{\frac{n''_{\mathrm{C}}}{2}-2}\end{array}\right] \tag{80}$$

which is implicit in $\mathrm{Wi}''_{\mathrm{Ci}}$. Fig. 6 plots $\mathrm{Wi}''_{\mathrm{Ci}}$ *versus* n''_{C} parametrized with $\mathbb{N}_{2\infty}$. It can thus be used to find $\mathrm{Wi}''_{\mathrm{Ci}}$ graphically, and this can then be inserted into:

$$\frac{\Psi_{2\mathrm{i}}}{\Psi_{20}} = \left(1-\mathbb{N}_{2\infty}\right)\left[1+\mathrm{Wi}''^{2}_{\mathrm{C}}\right]^{\frac{n''_{\mathrm{C}}}{2}-1} + \mathbb{N}_{2\infty} \tag{81}$$

to get the ordinate value of the inflection, $\ln\Psi_{2\mathrm{i}}$, on the second normal stress coefficient curve. Substituting Eqs. (72) and (77) into Eq. (38) then evaluating at $\mathrm{Wi}''_{\mathrm{C}} = \mathrm{Wi}''_{\mathrm{Ci}}$ gives the tangent slope defined by Eq. (42):

$$\left(n''-2\right) = \mathrm{Wi}''_{\mathrm{Ci}}\frac{\left(1-\mathbb{N}_{2\infty}\right)\left(n''_{\mathrm{C}}-2\right)\mathrm{Wi}''_{\mathrm{Ci}}\left(1+\mathrm{Wi}''^{2}_{\mathrm{Ci}}\right)^{\frac{n''_{\mathrm{C}}}{2}-2}}{\left(1-\mathbb{N}_{2\infty}\right)\left[1+\mathrm{Wi}''^{2}_{\mathrm{Ci}}\right]^{\frac{n''_{\mathrm{C}}}{2}-1}+\mathbb{N}_{2\infty}} \tag{82}$$

then substituting the result into Eq. (45) [with $\dot{\gamma} = \mathrm{Wi}''_{\mathrm{Ci}}/\lambda''_{\mathrm{C}}$] gives:

$$m'' = \Psi_{2\mathrm{i}}\left(\frac{\mathrm{Wi}''_{\mathrm{Ci}}}{\lambda_{\mathrm{C}}}\right)^{\delta''} \tag{83}$$

where:

$$\delta'' \equiv \frac{\left(2-n''_{\mathrm{C}}\right)\mathrm{Wi}''^{2}_{\mathrm{Ci}}\left(1+\mathrm{Wi}''^{2}_{\mathrm{Ci}}\right)^{\left(n''_{\mathrm{C}}-4\right)/2}}{\left[1+\mathrm{Wi}''^{2}_{\mathrm{Ci}}\right]^{\left(n''_{\mathrm{C}}-2\right)/2}+\mathbb{N}_{2\infty}/\left(1-\mathbb{N}_{2\infty}\right)} \tag{84}$$

We use Eqs. (54), (55), (67), (68), (80) and (81) with Eqs. (56), (57), (69), (70), (82) and (83) to get the shear power-law constants, n and m, the first normal power-law constants, n' and m', and the second normal power-law constants, n'' and m'', that are consistent with the inflection tangent of a Carreau fluid. We illustrate the procedure to obtain these three sets of power-law constants in Section 5.1. We provide the discussions for the special case of $\eta_\infty = 0$, $\Psi_{1\infty} = 0$ and $\Psi_{2\infty} = 0$ above, after Eqs. (48), (60) and (75).

3.2. Oldroyd 8-constant model

We now turn our attention to a more general constitutive equation (see Eq. (9) in Subsection 1.2), one that predicts not only the viscosity, but also the first and second normal stress coefficients in steady shear flow. This Oldroyd 8-constant model, we will see, allows us to examine inflections in all three curves, $\eta(\dot{\gamma})$, $\Psi_1(\dot{\gamma})$ and $\Psi_2(\dot{\gamma})$.

For the Oldroyd 8-constant model, the steady shear viscosity curve has the form of Eq. (18). Differentiating it once gives:

$$\frac{d\left(\eta/\eta_0\right)}{d\,\mathrm{Wi}} = \frac{2\,\mathrm{Wi}\left(\sigma-1\right)}{\left[1+\mathrm{Wi}^2\right]^2} \tag{85}$$

or twice:

$$\frac{d^2\left(\eta/\eta_0\right)}{d\,\mathrm{Wi}^2} = \frac{2\left(\sigma-1\right)\left(1-3\,\mathrm{Wi}^2\right)}{\left[1+\mathrm{Wi}^2\right]^3} \tag{86}$$

Substituting Eqs. (18), (85) and (86) into Eq. (35) gives:

$$\frac{d^2\ln\left(\eta/\eta_0\right)}{d\left(\ln\mathrm{Wi}\right)^2} = \frac{4\,\mathrm{Wi}^2\left(\sigma-1\right)\left(1-\sigma\,\mathrm{Wi}^4\right)}{\left(1+\mathrm{Wi}^2\right)^2\left(1+\sigma\,\mathrm{Wi}^2\right)^2} \tag{87}$$

Setting Eq. (87) to zero then solving for Wi_{i} gives:

$$\mathrm{Wi}_{\mathrm{i}} \equiv \sqrt{\sigma_1}\dot{\gamma}_{\mathrm{i}} = \frac{1}{\sqrt[4]{\sigma}} \tag{88}$$

to which the corresponding inflection viscosity is:

$$\frac{\eta_{\mathrm{i}}}{\eta_0} \equiv \frac{\eta\left(\mathrm{Wi}_{\mathrm{i}}\right)}{\eta_0} = \sqrt{\sigma} \tag{89}$$

and thus, the steady shear viscosity will inflect at the point:

$$\left(\mathrm{Wi}_{\mathrm{i}}, \frac{\eta_{\mathrm{i}}}{\eta_0}\right) = \left(\frac{1}{\sqrt[4]{\sigma}}, \sqrt{\sigma}\right) \tag{90}$$

For multiple relaxation times, using the same procedure to obtain Eq. (87), we get:

$$\frac{d^2\ln\left(\eta/\eta_0\right)}{d\left(\ln\mathrm{Wi}\right)^2} = \sum_{n=1}^{\infty}\frac{4\frac{\sigma_{1n}}{\sigma_1}\mathrm{Wi}^2\left(\sigma_n-1\right)\left(1-\frac{\sigma_{1n}^2\sigma_n}{\sigma_1^2}\mathrm{Wi}^4\right)}{\left(1+\frac{\sigma_{1n}}{\sigma_1}\mathrm{Wi}^2\right)^2\left(1+\frac{\sigma_{1n}\sigma_n}{\sigma_1}\mathrm{Wi}^2\right)^2} \tag{91}$$

where the *n-th Oldroyd shear thinning constant* is given by:

$$\sigma_{1n} \equiv \lambda_{1n}^2 + \mu_0\left(\mu_1-\tfrac{3}{2}\nu_1\right) - \mu_1\left(\mu_1-\nu_1\right) \tag{92}$$

and *n-th Oldroyd shear thickening constant*, by:

$$\sigma_{2n} \equiv \lambda_{1n}\lambda_2 + \mu_0\left(\mu_2-\tfrac{3}{2}\nu_2\right) - \mu_1\left(\mu_2-\nu_2\right) \tag{93}$$

and thus, the *n-th Oldroyd constant ratio*, by:

$$\sigma_n \equiv \frac{\sigma_{2n}}{\sigma_{1n}} = \frac{\lambda_{1n}\lambda_2 + \mu_0\left(\mu_2-\tfrac{3}{2}\nu_2\right) - \mu_1\left(\mu_2-\nu_2\right)}{\lambda_{1n}^2 + \mu_0\left(\mu_1-\tfrac{3}{2}\nu_1\right) - \mu_1\left(\mu_1-\nu_1\right)} \tag{94}$$

and finally, where the longest relaxation time is given by:

$$\sigma_{11} \equiv \sigma_1 = \lambda_1^2 + \mu_0\left(\mu_1-\tfrac{3}{2}\nu_1\right) - \mu_1\left(\mu_1-\nu_1\right) \tag{95}$$

Setting Eq. (91) to zero gives:

$$\sum_{n=1}^{\infty}\frac{4\frac{\sigma_{1n}}{\sigma_1}\mathrm{Wi}_{\mathrm{i}}^{\,2}\left(\sigma_n-1\right)\left(1-\frac{\sigma_{1n}^2\sigma_n}{\sigma_1^2}\mathrm{Wi}_{\mathrm{i}}^{\,4}\right)}{\left(1+\frac{\sigma_{1n}}{\sigma_1}\mathrm{Wi}_{\mathrm{i}}^{\,2}\right)^2\left(1+\frac{\sigma_{1n}\sigma_n}{\sigma_1}\mathrm{Wi}_{\mathrm{i}}^{\,2}\right)^2} = 0 \tag{96}$$

which defines the inflection Weissenberg number, Wi_{i}, implicitly.

Substituting Eqs. (18) and (85) into Eq. (32) gives the slope of the steady shear viscosity curve:

$$\frac{d\ln\left(\eta/\eta_0\right)}{d\ln\mathrm{Wi}} = \mathrm{Wi}\frac{1+\mathrm{Wi}^2}{1+\sigma\,\mathrm{Wi}^2}\frac{2\,\mathrm{Wi}\left(\sigma-1\right)}{\left(1+\mathrm{Wi}^2\right)^2} \tag{97}$$

and, Eq. (88) into Eq. (97) gives the inflection tangent slope:

$$(n-1)=\frac{-2\left(1-\sqrt{\sigma}\right)}{1+\sqrt{\sigma}} \tag{98}$$

where n is the shear power-law index. Eq. (98) thus allows us to deduce the shear power-law index from the Oldroyd 8-constant model parameters:

$$n=1-2\,\frac{1-\sqrt{\sigma}}{1+\sqrt{\sigma}} \tag{99}$$

which is a main result of this paper. Substituting Eq. (99) and the expression for the inflection point, Eq. (90), into Eq. (43) gives the expression for the shear power-law coefficient:

$$m=\eta_0\sqrt{\sigma}\left[\sigma_1\sqrt{\sigma}\right]^{-\frac{1-\sqrt{\sigma}}{1+\sqrt{\sigma}}} \tag{100}$$

Taking the limit as $\mathrm{Wi}\to\infty$ of Eq. (18) gives:

$$\frac{\eta_\infty}{\eta_0}\equiv\lim_{\mathrm{Wi}\to\infty}\frac{\eta}{\eta_0}=\sigma \tag{101}$$

Thus, for the special case $\sigma=0$, Eq. (18) approaches:

$$\frac{\eta}{\eta_0}=\frac{1}{1+\mathrm{Wi}^2} \tag{102}$$

asymptotically. For the special case of corotational Jeffreys, Eq. (101) reduces to:

$$\frac{\eta_\infty}{\eta_0}=\frac{\lambda_2}{\lambda_1} \tag{103}$$

and, for its special case, corotational Maxwell, to:

$$\frac{\eta_\infty}{\eta_0}=0 \tag{104}$$

For the special case $\sigma=0$, that is, where $\eta_\infty=0$, Eq. (18) predicts a double-valued τ_{yx}, and it approaches:

$$\frac{\eta}{\eta_0}=\frac{1}{\mathrm{Wi}^2}=\frac{1}{\sigma_1\dot{\gamma}^2} \tag{105}$$

asymptotically. Since $\tau_{yx}=\eta\dot{\gamma}$, substituting Eq. (105) into $\tau_{yx}=\eta\dot{\gamma}$ and differentiating gives:

$$\frac{d\tau}{d\dot{\gamma}}=\frac{-\eta_0}{\sigma_1\dot{\gamma}^2} \tag{106}$$

whence, we learn that, for the special case $\sigma=0$, for the Oldroyd 8-constant model, we identify the *unphysical* shear power-law index, n, with −1. By unphysical, we mean that, since we require that $d\tau_{yx}/d\dot{\gamma}>0$, n cannot be negative.

For the special case of the corotational Jeffreys model [see Eq. 7.3-3 of Bird *et al.* (1977); see also Eq. (1) of Subsection 14.423 of Jeffreys (1924 or 1929)], Eqs. (99), (100) reduce to:

$$n=1-2\,\frac{\sqrt{\lambda_1}-\sqrt{\lambda_2}}{\sqrt{\lambda_1}+\sqrt{\lambda_2}} \tag{107}$$

and:

$$m=\eta_0\sqrt{\frac{\lambda_2}{\lambda_1}}\left({\lambda_1}^3\lambda_2\right)^{\frac{1}{2}\frac{\sqrt{\lambda_1}-\sqrt{\lambda_2}}{\sqrt{\lambda_1}+\sqrt{\lambda_2}}} \tag{108}$$

and for its special case, the corotational Maxwell model, to:

$$n=-1 \tag{109}$$

and

$$m=\frac{\eta_0}{{\lambda_1}^2} \tag{110}$$

as it should.

For the Oldroyd 8-constant model, the first normal stress coefficient curve has the form of Eq. (22). Differentiating it once gives:

$$\frac{d\left(\Psi_1/\Psi_{10}\right)}{d\,\mathrm{Wi}}=\frac{-2\,\mathrm{Wi}\left(1-\sigma\right)\lambda_1}{\left(1+\mathrm{Wi}^2\right)^2\left(\lambda_1-\lambda_2\right)} \tag{111}$$

or twice:

$$\frac{d^2\left(\Psi_1/\Psi_{10}\right)}{d\,\mathrm{Wi}^2}=\frac{2\lambda_1\left(-1+3\,\mathrm{Wi}^2\right)\left(1-\sigma\right)}{\left(1+\mathrm{Wi}^2\right)^3\left(\lambda_1-\lambda_2\right)} \tag{112}$$

Substituting Eqs. (22), (111) and (112) into Eq. (37) gives:

$$\frac{d^2\ln\left(\Psi_1/\Psi_{10}\right)}{d\left(\ln\mathrm{Wi}\right)^2}=\frac{4\left(-\lambda_1+\lambda_1\sigma\,\mathrm{Wi}^4+\lambda_2-\lambda_2\,\mathrm{Wi}^4\right)\left(1-\sigma\right)\lambda_1\,\mathrm{Wi}^2}{\left(\lambda_1+\lambda_1\sigma\,\mathrm{Wi}^2-\lambda_2-\lambda_2\,\mathrm{Wi}^2\right)^2\left(1+\mathrm{Wi}^2\right)^2} \tag{113}$$

Setting Eq. (113) to zero, then solving for Wi_i gives:

$$\mathrm{Wi}_\mathrm{i}\equiv\sqrt{\sigma_1}\dot{\gamma}_\mathrm{i}=\sqrt[4]{\frac{\beta}{\alpha}} \tag{114}$$

where:

$$\alpha\equiv\lambda_1\sigma-\lambda_2 \tag{115}$$

and:

$$\beta\equiv\lambda_1-\lambda_2 \tag{116}$$

to which the corresponding inflection first normal stress coefficient is:

$$\frac{\Psi_{1\mathrm{i}}}{\Psi_{10}}\equiv\frac{\Psi_1\left(\mathrm{Wi}_\mathrm{i}\right)}{\Psi_{10}}=\sqrt{\frac{\alpha}{\beta}} \tag{117}$$

and thus, the first normal stress coefficient will inflect at the point:

$$\left(\mathrm{Wi}_\mathrm{i},\frac{\Psi_{1\mathrm{i}}}{\Psi_{10}}\right)=\left(\sqrt[4]{\frac{\beta}{\alpha}},\sqrt{\frac{\alpha}{\beta}}\right) \tag{118}$$

For multiple relaxation times, using the same procedure to obtain Eq. (113), we get:

$$\frac{d^2\ln\left(\Psi_1/\Psi_{10}\right)}{d\left(\ln\mathrm{Wi}\right)^2}=\sum_{n=1}^{\infty}\frac{4\left(-\lambda_{1n}+\lambda_2+\left(\lambda_{1n}\sigma_n-\lambda_2\right)\frac{\sigma_{1n}^2}{\sigma_1^2}\mathrm{Wi}^4\right)\left(1-\sigma_n\right)\lambda_{1n}\frac{\sigma_{1n}}{\sigma_1}\mathrm{Wi}^2}{\left(\lambda_{1n}-\lambda_2+\left(\lambda_{1n}\sigma_n-\lambda_2\right)\frac{\sigma_{1n}}{\sigma_1}\mathrm{Wi}^2\right)^2\left(1+\frac{\sigma_{1n}}{\sigma_1}\mathrm{Wi}^2\right)^2} \tag{119}$$

where the n-th Oldroyd shear thinning, shear thickening constants and the n-th Oldroyd constant ratio, σ_{1n}, σ_{2n} and σ_n are given by Eqs. (92)-(94). Setting Eq. (119) to zero gives:

$$\sum_{n=1}^{\infty}\frac{4\left(-\lambda_{1n}+\lambda_2+\left(\lambda_{1n}\sigma_n-\lambda_2\right)\frac{\sigma_{1n}^2}{\sigma_1^2}\mathrm{Wi_i}^4\right)\left(1-\sigma_n\right)\lambda_{1n}\frac{\sigma_{1n}}{\sigma_1}\mathrm{Wi_i}^2}{\left(\lambda_{1n}-\lambda_2+\left(\lambda_{1n}\sigma_n-\lambda_2\right)\frac{\sigma_{1n}}{\sigma_1}\mathrm{Wi_i}^2\right)^2\left(1+\frac{\sigma_{1n}}{\sigma_1}\mathrm{Wi_i}^2\right)^2}=0 \quad (120)$$

which defines the inflection Weissenberg number, $\mathrm{Wi_i}$, implicitly.

Substituting Eqs. (22) and (111) into Eq. (36) gives the slope of the first normal stress coefficient curve:

$$\frac{d\ln\left(\Psi_1/\Psi_{10}\right)}{d\ln\mathrm{Wi}}=\frac{-2\,\mathrm{Wi}^2\left(1-\sigma\right)\lambda_1}{\left(\beta+\alpha\,\mathrm{Wi}^2\right)\left(1+\mathrm{Wi}^2\right)} \quad (121)$$

and, Eq. (114) into Eq. (121) gives the inflection tangent slope:

$$\left(n'-2\right)=\frac{-2\left(1-\sigma\right)\lambda_1}{\left(\sqrt{\alpha}+\sqrt{\beta}\right)^2} \quad (122)$$

where n' is the first normal power-law index. Eq. (122) thus allows us to deduce the first normal power-law index from the Oldroyd 8-constant model constants:

$$n'=2-2\frac{\left(1-\sigma\right)\lambda_1}{\left(\sqrt{\alpha}+\sqrt{\beta}\right)^2} \quad (123)$$

which is another main result of this paper. Substituting Eq. (123) and the expression for the inflection point, Eq. (118), into Eq. (44) gives the expression for the first normal power-law coefficient:

$$m'=\Psi_{10}\sqrt{\frac{\alpha}{\beta}}\left[\frac{\beta}{\alpha\sigma_1^2}\right]^{\frac{\lambda_1\left(1-\sigma\right)}{2\left(\sqrt{\alpha}+\sqrt{\beta}\right)^2}} \quad (124)$$

Substituting Eq. (18) into Eq. (22) then simplifying gives:

$$\frac{\Psi_1}{\Psi_{10}}=\frac{\left(\lambda_1-\lambda_2\right)+\left(\lambda_1\sigma-\lambda_2\right)\mathrm{Wi}^2}{\left(\lambda_1-\lambda_2\right)\left(1+\mathrm{Wi}^2\right)} \quad (125)$$

which, in the limit $\mathrm{Wi}\to\infty$, gives:

$$\frac{\Psi_{1\infty}}{\Psi_{10}}\equiv\lim_{\mathrm{Wi}\to\infty}\frac{\Psi_1}{\Psi_{10}}=\frac{\lambda_1\sigma-\lambda_2}{\lambda_1-\lambda_2} \quad (126)$$

Thus, for the special case:

$$\frac{\lambda_2}{\lambda_1}=\sigma=\frac{\lambda_1\lambda_2+\mu_0\left(\mu_2-\frac{3}{2}\nu_2\right)-\mu_1\left(\mu_2-\nu_2\right)}{\lambda_1^2+\mu_0\left(\mu_1-\frac{3}{2}\nu_1\right)-\mu_1\left(\mu_1-\nu_1\right)} \quad (127)$$

$\Psi_{1\infty}=0$. Eq. (125) approaches:

$$\frac{\Psi_1}{\Psi_{10}}=\frac{1}{\mathrm{Wi}^2} \quad (128)$$

asymptotically. For the special case of corotational Jeffreys, Eq. (126) reduces to:

$$\frac{\Psi_{1\infty}}{\Psi_{10}}=0 \quad (129)$$

and also the same for its special case, the corotational Maxwell model.

Substituting Eqs. (24), (99), (100), (123) and (124) into Eq. (4) gives the first inflection pairing time for the Oldroyd 8-constant model:

$$\lambda_{\mathrm{B}}'\equiv\left(\sqrt{\frac{\alpha\beta}{\sigma}}\left[\frac{\beta}{\alpha\sigma_1^2}\right]^{\frac{\lambda_1\left(1-\sigma\right)}{2\left(\sqrt{\alpha}+\sqrt{\beta}\right)^2}}\left[\sigma_1\sqrt{\sigma}\right]^{\frac{1-\sqrt{\sigma}}{1+\sqrt{\sigma}}}\right)^{\frac{\left(\sqrt{\alpha}+\sqrt{\beta}\right)^2\left(1+\sqrt{\sigma}\right)}{\left(3-\sqrt{\sigma}\right)\left(\sqrt{\alpha}+\sqrt{\beta}\right)^2-2\left(1-\sigma\right)\lambda_1\left(1+\sqrt{\sigma}\right)}} \quad (130)$$

For the corotational Jeffreys model, Eqs. (122), (124) and (130) reduce to:

$$\left(n'-2\right)=-2 \quad (131)$$

$$m'=\frac{\Psi_{10}}{\lambda_1^2} \quad (132)$$

$$\lambda_{\mathrm{B}}'=\left(\frac{\lambda_1-\lambda_2}{\sqrt{\lambda_1^3}\sqrt{\lambda_2}}\left[\lambda_1^2\sqrt{\frac{\lambda_2}{\lambda_1}}\right]^{\frac{\sqrt{\lambda_1}-\sqrt{\lambda_2}}{\sqrt{\lambda_1}+\sqrt{\lambda_2}}}\right)^{\frac{\sqrt{\lambda_1}+\sqrt{\lambda_2}}{\sqrt{\lambda_1}-3\sqrt{\lambda_2}}} \quad (133)$$

and for its special case, the corotational Maxwell model, to:

$$\left(n'-2\right)=-2 \quad (134)$$

$$m'=\frac{\Psi_{10}}{\lambda_1^2} \quad (135)$$

$$\lambda_{\mathrm{B}}'=\lambda_1 \quad (136)$$

The product of the first inflection pairing time and the shear power-law index, $n\lambda_{\mathrm{B}}'$, has been used to scale the time for squeeze flow measurements [see Fig. 5.2-5 of EXAMPLE 5.2-6 of Bird *et al.* (1977)]. Specifically, at times falling below $n\lambda_{\mathrm{B}}'$, *quasi-steady state* solutions fail. By quasi-steady state, we mean locally, instantaneously steady flow [see Paragraph a. in EXAMPLE 5.2-6 of Bird *et al.* (1977)]. This is why Eq. (130) is also a main result of this work.

For the Oldroyd 8-constant model, the second normal stress coefficient curve has the form of Eq. (23). Differentiating it once gives:

$$\frac{d\left(\Psi_2/\Psi_{20}\right)}{d\,\mathrm{Wi}}=\frac{-2\,A\left(1-\sigma\right)\mathrm{Wi}}{\left(A-B\right)\left(1+\mathrm{Wi}^2\right)^2} \quad (137)$$

or twice:

$$\frac{d^2\left(\Psi_2/\Psi_{20}\right)}{d\,\mathrm{Wi}^2}=\frac{-2A\left(1-\sigma\right)\left(1-3\,\mathrm{Wi}^2\right)}{\left(A-B\right)\left(1+\mathrm{Wi}^2\right)^3} \quad (138)$$

where:

$$A\equiv\lambda_1-\mu_1 \quad (139)$$

and:

$$B \equiv \lambda_2 - \mu_2 \tag{140}$$

Substituting Eqs. (23), (137) and (138) into Eq. (39) gives:

$$\frac{d^2 \ln\left(\Psi_2/\Psi_{20}\right)}{d\left(\ln \mathrm{Wi}\right)^2} = \frac{-4A\left(1-\sigma\right)\left[A-B-\left(A\sigma-B\right)\mathrm{Wi}^4\right]\mathrm{Wi}^2}{\left[A-B+\left(A\sigma-B\right)\mathrm{Wi}^2\right]^2\left(1+\mathrm{Wi}^2\right)^2} \tag{141}$$

Setting Eq. (141) to zero then solving for Wi_i gives:

$$\mathrm{Wi}_\mathrm{i} \equiv \sqrt{\sigma_1}\dot{\gamma}_\mathrm{i} = \sqrt[4]{\frac{A-B}{A\sigma-B}} \tag{142}$$

to which the corresponding inflection of the second normal stress coefficient is:

$$\frac{\Psi_{2\mathrm{i}}}{\Psi_{20}} \equiv \frac{\Psi_2\left(\mathrm{Wi}_\mathrm{i}\right)}{\Psi_{20}} = \sqrt{\frac{A\sigma-B}{A-B}} \tag{143}$$

and thus, the second normal stress coefficient will inflect at the point:

$$\left(\mathrm{Wi}_\mathrm{i}, \frac{\Psi_{2\mathrm{i}}}{\Psi_{20}}\right) = \left(\sqrt[4]{\frac{A-B}{A\sigma-B}}, \sqrt{\frac{A\sigma-B}{A-B}}\right) \tag{144}$$

For multiple relaxation times, using the same procedure to obtain Eq. (141), we get:

$$\frac{d^2 \ln\left(\Psi_2/\Psi_{20}\right)}{d\left(\ln \mathrm{Wi}\right)^2} = \sum_{n=1}^{\infty} \frac{-4A_n\left(1-\sigma_n\right)\left[A_n - B - \left(A_n\sigma_n - B\right)\frac{\sigma_{1n}^2}{\sigma_1^2}\mathrm{Wi}^4\right]\frac{\sigma_{1n}}{\sigma_1}\mathrm{Wi}^2}{\left[A_n - B + \left(A_n\sigma_n - B\right)\frac{\sigma_{1n}}{\sigma_1}\mathrm{Wi}^2\right]^2\left(1+\frac{\sigma_{1n}}{\sigma_1}\mathrm{Wi}^2\right)^2} \tag{145}$$

where:

$$A_n \equiv \lambda_{1n} - \mu_1 \tag{146}$$

and where the n-th Oldroyd shear thinning, shear thickening constants and the n-th Oldroyd constant ratio, σ_{1n}, σ_{2n} and σ_n are given by Eqs. (92)-(94). Setting Eq. (145) to zero gives:

$$\sum_{n=1}^{\infty} \frac{-4A_n\left(1-\sigma_n\right)\left[A_n - B - \left(A_n\sigma_n - B\right)\frac{\sigma_{1n}^2}{\sigma_1^2}\mathrm{Wi}_\mathrm{i}^4\right]\frac{\sigma_{1n}}{\sigma_1}\mathrm{Wi}_\mathrm{i}^2}{\left[A_n - B + \left(A_n\sigma_n - B\right)\frac{\sigma_{1n}}{\sigma_1}\mathrm{Wi}_\mathrm{i}^2\right]^2\left(1+\frac{\sigma_{1n}}{\sigma_1}\mathrm{Wi}_\mathrm{i}^2\right)^2} = 0 \tag{147}$$

which defines the inflection Weissenberg number, Wi_i, implicitly.

Substituting Eqs. (23) and (137) into Eq. (38) gives the slope of the second normal stress coefficient curve:

$$\frac{d\ln\left(\Psi_2/\Psi_{20}\right)}{d\ln\left(\lambda\dot{\gamma}\right)} = \frac{-2A\left(1-\sigma\right)\mathrm{Wi}^2}{\left(1+\mathrm{Wi}^2\right)\left[A-B+\left(A\sigma-B\right)\mathrm{Wi}^2\right]} \tag{148}$$

and, Eq. (142) into Eq. (148) gives the inflection tangent slope:

$$\left(n''-2\right) = \frac{-2\left(1-\sigma\right)A}{\left(\sqrt{A-B}+\sqrt{A\sigma-B}\right)^2} \tag{149}$$

and where n'' is the second normal power-law index. Eq. (149) thus allows us to deduce the second normal power-law index from the Oldroyd 8-constant model constants:

$$n'' = 2 - \frac{2\left(1-\sigma\right)A}{\left(\sqrt{A-B}+\sqrt{A\sigma-B}\right)^2} \tag{150}$$

which is another main result of this paper. Substituting Eq. (150) and the expression for the inflection point Eq. (144) into Eq. (45) gives the expression for the second normal power-law coefficient:

$$m'' = -\Psi_{20}\sqrt{\frac{A\sigma-B}{A-B}}\left[\frac{A-B}{\left(A\sigma-B\right)\sigma_1^2}\right]^{\frac{(1-\sigma)A}{2\left(\sqrt{A-B}+\sqrt{A\sigma-B}\right)^2}} \tag{151}$$

Substituting Eq. (18) into Eq. (23) then simplifying gives:

$$\frac{\Psi_2}{\Psi_{20}} = \frac{\left(\lambda_1-\lambda_2-\mu_1+\mu_2\right)+\left(\lambda_1\sigma-\lambda_2-\mu_1\sigma+\mu_2\right)\mathrm{Wi}^2}{\left(\lambda_1-\lambda_2-\mu_1+\mu_2\right)\left(1+\mathrm{Wi}^2\right)} \tag{152}$$

which, in the limit $\mathrm{Wi}\to\infty$, gives:

$$\frac{\Psi_{2\infty}}{\Psi_{20}} \equiv \lim_{\mathrm{Wi}\to\infty}\frac{\Psi_2}{\Psi_{20}} = \frac{\lambda_1\sigma-\lambda_2-\mu_1\sigma+\mu_2}{\lambda_1-\lambda_2-\mu_1+\mu_2} \tag{153}$$

Thus, for the special case:

$$\lambda_1\sigma-\lambda_2-\mu_1\sigma+\mu_2 = 0 \tag{154}$$

$\Psi_{2\infty} = 0$. Eq. (152) approaches:

$$\frac{\Psi_2}{\Psi_{20}} = \frac{1}{\mathrm{Wi}^2} \tag{155}$$

asymptotically. For the special case of corotational Jeffreys, Eq. (153) reduces to:

$$\frac{\Psi_{2\infty}}{\Psi_{20}} = 0 \tag{156}$$

and also the same for its special case, the corotational Maxwell model.

Substituting Eqs. (25), (99), (100), (150) and (151) into Eq. (5) gives:

$$\lambda_\mathrm{B}'' \equiv \left(\frac{m''}{2m}\right)^{1/(n''-n)} \tag{5}$$

where:

$$\frac{1}{n''-n} = \frac{\left(1+\sqrt{\sigma}\right)\left(\sqrt{A-B}+\sqrt{A\sigma-B}\right)^2}{\left(3-\sqrt{\sigma}\right)\left(\sqrt{A-B}+\sqrt{A\sigma-B}\right)^2 - 2\left(1-\sigma\right)\left(1+\sqrt{\sigma}\right)A} \tag{157}$$

and:

$$\frac{m''}{2m} = \frac{1}{2}\sqrt{\frac{\left(A-B\right)\left(A\sigma-B\right)}{\sigma}}\left[\frac{A-B}{{\sigma_1}^2\left(A\sigma-B\right)}\right]^{\frac{(1-\sigma)A}{2\left(\sqrt{A-B}+\sqrt{A\sigma-B}\right)^2}} \times\left[\sigma_1\sqrt{\sigma}\right]^{\frac{1-\sqrt{\sigma}}{1+\sqrt{\sigma}}} \tag{158}$$

For the corotational Jeffreys model, Eqs. (149), (151) and (5) [with Eqs. (157) and (158)] reduce to:

$$(n''-2) = -2 \tag{159}$$

$$m'' = \eta_0 \frac{(\lambda_1 - \lambda_2)}{{\lambda_1}^2} \tag{160}$$

$$\lambda_B'' = \left[\frac{1}{2} \frac{\lambda_1 - \lambda_2}{\sqrt{\lambda_1^3 \lambda_2}} \left(\sqrt{\lambda_1^3 \lambda_2} \right)^{\frac{\sqrt{\lambda_1}-\sqrt{\lambda_2}}{\sqrt{\lambda_1}+\sqrt{\lambda_2}}} \right]^{\frac{\sqrt{\lambda_1}+\sqrt{\lambda_2}}{\sqrt{\lambda_1}-3\sqrt{\lambda_2}}} \tag{161}$$

and for its special case, the corotational Maxwell model, to:

$$(n''-2) = -2 \tag{162}$$

$$m'' = \frac{\eta_0}{\lambda_1} \tag{163}$$

$$\lambda_B'' = \frac{\lambda_1}{2} \tag{164}$$

Whereas λ_B' is known as the characteristic time for the quasi-periodicity, no one has ever measured or calculated λ_B''. Its usefulness is unexplored.

4. Conclusion

Even though the inflection slope of the steady shear viscosity can govern polymer extrusion productivity, we find no articles on inflection *per se*. We have thus explored inflections in the viscometric functions, and specifically, inflection in the log-log curves *versus* shear rate. For this exploration, we chose the Carreau and the Oldroyd 8-constant models. For these viscometric functions we included the viscosity curve and both curves on normal stress difference coefficient.

In Section 2, we derived expressions for both first and second derivatives on logarithm scale for all three viscometric functions: (1) steady shear viscosity, η, (2) steady shear first normal stress coefficient, Ψ_1, and (3) steady shear second normal stress coefficient, Ψ_2. We then used these results in Section 3 to determine the inflection tangents, and from these, the corresponding power-law indexes and power-law coefficients, for both the Carreau and the Oldroyd 8-constant models.

From the Carreau viscosity model, in Eqs. (7) and (8), we propose expressions of the same form, for the first and second normal stress coefficients. We then find that the inflection Weissenberg number, Wi_i, for all three viscometric functions to be implicit [see Eqs. (54), (67) and (80)]. In Subsection 3.1, we discuss the special cases, $\eta_\infty = 0$, $\Psi_{1\infty} = 0$ and $\Psi_{2\infty} = 0$.

For the Oldroyd 8-constant model, we calculate expressions for the inflection points in Eqs. (90), (118) and (144). We use these points to find inflection tangents, and the corresponding power-law indexes, n, n' and n'' [see Eqs. (99), (123) and (150)], the main results of this paper. We also provide expressions for the power-law coefficients, m, m' and m'' [see Eqs. (100), (124) and (151)]. As consistency checks, we reduce our answers for the Oldroyd 8-constant model to two simpler special cases, the corotational Jeffreys and corotational Maxwell models. We end with a discussion of the first and second inflection pairing times, λ_B' and λ_B'', with which the Leider number is defined. The Leider number, Ld, is used to determine the applicability of the quasi-steady state solutions [Eq. (2) of Leider (1974) or Eq. (20) of Leider and Bird (1974)].

We find no experimental data for all three viscometric functions, $\eta(\dot{\gamma})$, $\Psi_1(\dot{\gamma})$ and $\Psi_2(\dot{\gamma})$, on the same material. In the Worked Example 5.1, for the Carreau fluid, we fit the models [Eqs. (46) and (59)] to $\eta(\dot{\gamma})$ and $\Psi_1(\dot{\gamma})$ measurements on a polyisobutylene solution. For the corotational Jeffreys model (special case of Oldroyd 8-constant), we use a spectrum of relaxation times employing the Spriggs relations [Eqs. (180) and (181)] and our own corresponding spectral relation for the retardation time [Eq. (182)] to get a good fit for $\eta(\dot{\gamma})$. We close with Worked Examples that illustrate how to calculate n, n', m, m' and λ_B' for both the Carreau and corotational Jeffreys, and then how to use the Leider number.

Whereas log-log plots of viscosity *versus* shear rate will inflect at Wi_i, the linear-linear plot of viscosity *versus* shear rate will, of course, inflect at Weissenberg number well below Wi_i. We close by noting that reflections on these linear-linear inflections, though beyond the scope of this paper, might be equally interesting.

5. Worked Examples: Finding Inflections

A factory processes a polyisobutylene solution, 2.0% by weight, in Primol™ white oil. An engineer is using her *quasi-steady state* solution to predict throughput. The characteristic flow time for her polymer processing problem is roughly $t_p \approx 100\mathrm{s}$. She wonders if her quasi-steady state solution will apply.

To address this question, she must calculate the *Leider number*:

$$\mathrm{Ld} \equiv \frac{n\lambda'}{t_p} \tag{165}$$

If $\mathrm{Ld} > 1$, then she can expect her quasi-steady state solution to work [see EXAMPLE 5.2-6 of Bird *et al.* (1977); Section 10.2.2., Example 10.4 and 10.5 of Baird and Collias (1998 and 2014)]. She first extracts the data from Fig. 4.3-3 of Bird *et al.* (1977) for the steady shear viscosity, and from Fig. 4.3-6 of Bird *et al.* (1977) for the first normal stress coefficient. She calculates the tangent slope for both the steady shear viscosity, $(n-1)$, and the first normal stress coefficient, $(n'-2)$. She does this for both the Carreau and the Oldroyd 8-constant models.

5.1. Carreau model

The engineer fits Eq. (46) to the 36 steady shear vis-

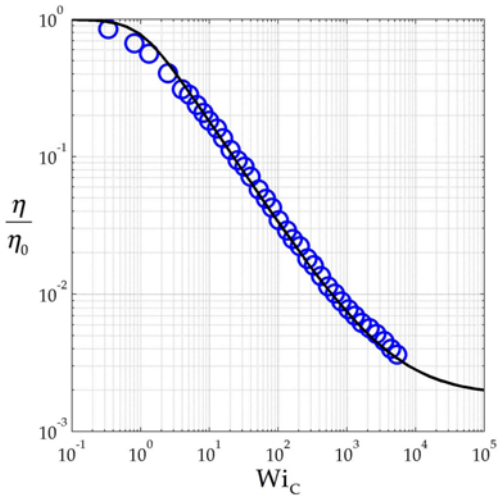

Fig. 7. Best fit of Carreau model (Black curve) [Eq. (46)] with $\eta_0 = 1.10\times10^3$ Pa·s, $\eta_\infty = 2.00$ Pa·s, $\lambda_C = 150.$s and $n_C = 0.250$ to data from Fig. 4.3-3 of Bird *et al.* (1977) for 2.0% by weight polyisobutylene solution in Primol™ white oil (Blue circles).

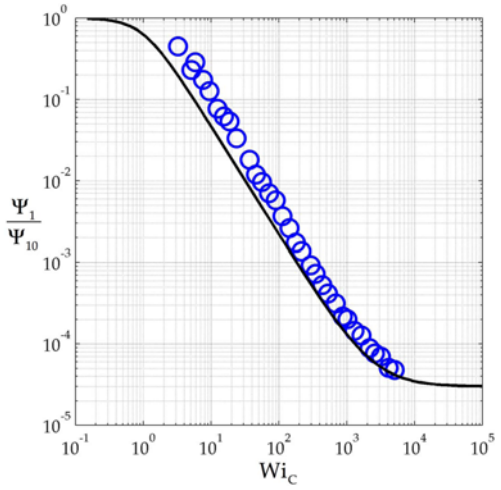

Fig. 8. Forced through $\lambda_C' = \lambda_C = 150.$s, the best fit of the Carreau model [Eq. (46)] (Black curve) [Eq. (59)] with $\Psi_{10} = 1.00\times10^5$ Pa·s^2, $\Psi_{1\infty} = 3.00$ Pa·s^2 and $n_C' = 0.667$ to data from Fig. 4.3-6 of Bird *et al.* (1977) for 2.0% by weight polyisobutylene solution in Primol™ white oil (Blue circles).

cosity measurements from Fig. 4.3-3 of Bird *et al.* (1977), and gets $\eta_0 = 1.10\times10^3$ Pa·s, $\eta_\infty = 2.00$ Pa·s, $\lambda_C = 150.$ s and $n_C = 0.250$ (see Fig. 7). To calculate the tangent slope of the steady shear viscosity, $(n-1)$, she substitutes these best-fit parameters into Eq. (47) to get:

$$\mathbb{H}_\infty = \frac{2.00\ \text{Pa}\cdot\text{s}}{1.10\times10^3\ \text{Pa}\cdot\text{s}} = \frac{1}{550.} \tag{166}$$

Using her best-fit shear Carreau index, n_C, together with Eq. (166), she then interpolates using Fig. 5 to get:

$$Wi_{Ci} = 14.2 \tag{167}$$

Substituting n_C, Eqs. (166) and (167) into Eq. (55) gives:

$$\eta_i = 1.10\times10^3\ \text{Pa}\cdot\text{s}\left\{\left[1-\frac{1}{550.}\right]\left[1+14.2^2\right]^{(0.250-1)/2}+\frac{1}{550.}\right\} = 152\ \text{Pa}\cdot\text{s} \tag{168}$$

the ordinate value corresponding to the inflection Weissenberg number. Substituting Eqs. (167) and (168) into Eq. (56) gives:

$$(n-1) = 14.2\frac{\left(1-\frac{1}{550.}\right)(0.250-1)14.2\left(1+14.2^2\right)^{\frac{0.250-3}{2}}}{\left(1-\frac{1}{550.}\right)\left[1+14.2^2\right]^{(0.250-1)/2}+\frac{1}{550.}} = -0.737 \tag{169}$$

thus:

$$n = 0.264 \tag{170}$$

Substituting Eqs. (167) and (168) into Eq. (57) gives:

$$m = 152.\ \text{Pa}\cdot\text{s}\left(\frac{14.2}{150.\text{s}}\right)^{-(-0.737)} = 26.8\ \text{Pa}\cdot\text{s}^n \tag{171}$$

To match the characteristic times for Eqs. (46) and (59), she forces the fit of Eq. (59) through $\lambda_C' = \lambda_C = 150.$ s. For this fit of Eq. (59) to the 32 first normal stress coefficient measurements, she gets $\Psi_{10} = 1.00\times10^5$ Pa·s^2, $\Psi_{1\infty} = 3.00$ Pa·s^2 and $n_C' = 0.667$ (see Fig. 8). To calculate the tangent slope of the first normal stress coefficient, $(n'-2)$, she substitutes these best-fit parameters into Eq. (60) to get:

$$\mathbb{N}_{1\infty} \equiv \frac{3.00\ \text{Pa}\cdot\text{s}^2}{1.00\times10^5\ \text{Pa}\cdot\text{s}^2} = 3.00\times10^{-5} \tag{172}$$

Using her best-fit first normal Carreau index, n_C', together with Eq. (172), she then interpolates using Fig. 6 to get:

$$Wi_{Ci}' = 25.7 \tag{173}$$

Substituting n_C', Eqs. (172) and (173) into Eq. (68) gives:

$$\Psi_{1i} = 1.00\times10^5\ \text{Pa}\cdot\text{s}^2 \times\left\{\left[1-3.00\times10^{-5}\right]\left[1+25.7^2\right]^{\frac{0.667}{2}-1}+3.00\times10^{-}\right. = 1320\ \text{Pa}\cdot\text{s}^2 \tag{174}$$

the ordinate value corresponding to the inflection Weissenberg number. Substituting Eqs. (173) and (174) into Eq. (69) gives:

$$(n'-2) = 25.7\frac{\left(1+3.00\times10^{-5}\right)(0.667-2)25.7\left(1+25.7^2\right)^{\frac{0.667}{2}-2}}{\left(1-\frac{3}{10^5}\right)\left[1+25.7^2\right]^{\frac{0.667}{2}-1}+3.00\times10^{-5}} = -1.33 \tag{175}$$

thus:

$$n' = 0.672 \tag{176}$$

Substituting Eqs. (173) and (174) into Eq. (70) gives:

$$m' = 1320\ \text{Pa}\cdot\text{s}^2\left(\frac{25.7}{150.\text{s}}\right)^{-(-1.33)} = 127.\ \text{Pa}\cdot\text{s}^{n'} \tag{177}$$

She then calculate the Leider number, Ld. Substituting λ_C' = 150. s, $t_p \approx 100$s and Eq. (170) into Eq. (165) gives:

$$\mathrm{Ld} \approx \frac{0.264(150.\mathrm{s})}{100.\mathrm{s}} = 0.396 < 1 \tag{178}$$

thus, she can expect her quasi-steady state solution to apply.

5.2. Corotational Jeffreys model, multiple λ_1 and λ_2

She first simplifies the Oldroyd 8-constant model to the corotational Jeffreys model ($\mu_0 = \mu_1 = \mu_2 = \nu_1 = \nu_2 = 0$) and then generalized with the *discrete Jeffreys spectrum* following Eqs. (180)-(182). She then examines the steady shear viscosity curve for the corotational Jeffreys model. The steady shear viscosity for multiple relaxation times is given by:

$$\eta = \sum_{k=1}^{\infty} \frac{1 + \frac{\lambda_{2k}}{\lambda_{1k}} (\lambda_{1k}\dot{\gamma})^2}{1 + (\lambda_{1k}\dot{\gamma})^2} \eta_k \tag{179}$$

where η_k is given by the *first Spriggs relation* [Eq. (6.1-14) in Bird *et al.* (1977)]:

$$\eta_k \equiv \frac{\eta_0 \lambda_{1k}}{\sum_k \lambda_{1k}} \tag{180}$$

and where the λ_{1k} is given by the *second Spriggs relation* [Eq. (6.1-15) in Bird *et al.* (1977)]:

$$\lambda_{1k} = \frac{\lambda_1}{k^{\alpha_t}} \tag{181}$$

and also, we propose, where:

$$\lambda_{2k} = \frac{\lambda_2}{k^{\alpha_t}} \tag{182}$$

where λ_1 and λ_2 are the longest relaxation and longest retardation times. We call (η_k, λ_{1k}, λ_{2k}) the *discrete Jeffreys spectrum*, and Eqs. (180)-(182) the *Spriggs relations for the discrete Jeffreys spectrum.* From Eqs. (181) and (182), we learn that α_t governs the separation of the relaxation and retardation times. Substituting Eq. (181) into Eq. (180) gives:

$$\eta_k = \frac{\eta_0}{k^{\alpha_t} \sum_k \frac{1}{k^{\alpha_t}}} = \frac{\eta_0}{k^{\alpha_t} \zeta(\alpha_t)} \tag{183}$$

where the *Riemann zeta function* is defined by [see Eq. 23.2.1 in Abramowitz and Stegun (1970)]:

$$\zeta(\alpha_t) \equiv \sum_{k=1}^{\infty} \frac{1}{k^{\alpha_t}} \tag{184}$$

Substituting Eqs. (181)-(183) into Eq. (179) gives:

$$\eta = \frac{\eta_0}{\zeta(\alpha_t)} \sum_{k=1}^{\infty} \frac{k^{\alpha_t} + \frac{\lambda_2}{\lambda_1 k^{\alpha_t}} (\lambda_1\dot{\gamma})^2}{k^{2\alpha_t} + (\lambda_1\dot{\gamma})^2} \tag{185}$$

where:

$$\lim_{\lambda_1\dot{\gamma}\to 0} \eta = \frac{\eta_0}{\zeta(\alpha_t)} \lim_{\lambda_1\dot{\gamma}\to 0} \sum_{k=1}^{\infty} \frac{k^{\alpha_t} + \frac{\lambda_2}{\lambda_1 k^{\alpha_t}} (\lambda_1\dot{\gamma})^2}{k^{2\alpha_t} + (\lambda_1\dot{\gamma})^2} = \eta_0 \tag{186}$$

as it must, and where:

$$\lim_{\lambda\dot{\gamma}\to\infty} \eta \equiv \eta_\infty = \frac{\eta_0}{\zeta(\alpha_t)} \lim_{\lambda\dot{\gamma}\to\infty} \sum_{k=1}^{\infty} \frac{k^{\alpha_t} + \frac{\lambda_2}{\lambda_1 k^{\alpha_t}} (\lambda_1\dot{\gamma})^2}{k^{2\alpha_t} + (\lambda_1\dot{\gamma})^2} = \eta_0 \frac{\lambda_2}{\lambda_1} \tag{187}$$

which matches the result for a single λ_1 corotational Jeffreys fluid.

Adimensionalizing Eq. (185):

$$\frac{\eta}{\eta_0} = \frac{1}{\zeta(\alpha_t)} \sum_{k=1}^{\infty} \frac{k^{\alpha_t} + \frac{\lambda_2}{\lambda_1 k^{\alpha_t}} (\lambda_1\dot{\gamma})^2}{k^{2\alpha_t} + (\lambda_1\dot{\gamma})^2} \tag{188}$$

and differentiating once gives:

$$\frac{d(\eta/\eta_0)}{d(\lambda_1\dot{\gamma})} = \frac{2(\lambda_2 - \lambda_1)}{\lambda_1 \zeta(\alpha_t)} \sum_{k=1}^{\infty} \frac{k^{\alpha_t} (\lambda_1\dot{\gamma})}{\left[k^{2\alpha_t} + (\lambda_1\dot{\gamma})^2\right]^2} \tag{189}$$

or twice:

$$\frac{d^2(\eta/\eta_0)}{d(\lambda_1\dot{\gamma})^2} = \frac{2(\lambda_2 - \lambda_1)}{\lambda_1 \zeta(\alpha_t)} \sum_{k=1}^{\infty} \frac{k^{\alpha_t} \left(k^{2\alpha_t} - 3(\lambda_1\dot{\gamma})^2\right)}{\left(k^{2\alpha_t} + (\lambda_1\dot{\gamma})^2\right)^3} \tag{190}$$

The engineer fits Eq. (188) to the 36 steady shear viscosity measurements from Fig. 4.3-3 of Bird *et al.* (1977) [see also Huppler *et al.* (1967)]. Fig. 9 illustrates this best fit of the Oldroyd 8-constant model: $\eta_0 = 1.10 \times 10^3$ Pa·s, $\alpha_t = 2.70$, $\lambda_1 = 100.$s and $\lambda_2 = 0.100$s. Substituting Eqs. (188)-(190) into Eq. (35) gives:

$$\frac{d^2 \ln(\eta/\eta_0)}{d(\ln \lambda_1\dot{\gamma})^2} = \phi(\lambda_1\dot{\gamma})^2 \left[\left\{ 1 - \phi(\lambda_1\dot{\gamma})^2 \sum_{k=1}^{\infty} \frac{k^{\alpha_t}}{\Lambda_k^2} \right\} \sum_{k=1}^{\infty} \frac{k^{\alpha_t}}{\Lambda_k^2} + \sum_{k=1}^{\infty} \frac{k^{\alpha_t} \left(k^{2\alpha_t} - 3(\lambda_1\dot{\gamma})^2\right)}{\Lambda_k^3} \right] \tag{191}$$

where:

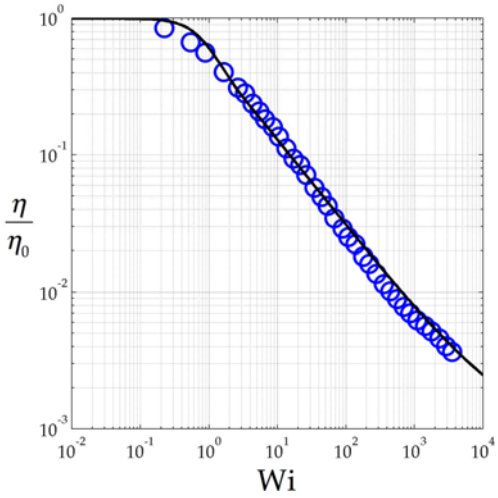

Fig. 9. Best fit of Oldroyd 8-constant model (Black curve) [Eq. (188)] with $\eta_0 = 1.10 \times 10^3$ Pa·s, $\alpha = 2.70$, $\lambda_1 = 100.$s and $\lambda_2 = 0.100$s to data from Fig. 4.3-6 of Bird *et al.* (1977) for 2.0% by weight polyisobutylene solution in Primol™ white oil (Blue circles).

$$\phi \equiv \frac{2(\lambda_2-\lambda_1)}{\lambda_1\sum_{k=1}^{\infty}\frac{k^{\alpha_t}+\frac{\lambda_2}{\lambda_1 k^{\alpha_t}}(\lambda_1\dot{\gamma})^2}{\Lambda_k}} \tag{192}$$

and:

$$\Lambda_k \equiv k^{2\alpha_t}+(\lambda_1\dot{\gamma})^2 \tag{193}$$

Setting Eq. (191) to zero gives the inflection Weissenberg number, $\mathrm{Wi_i} \equiv \lambda_1\dot{\gamma}_\mathrm{i}$:

$$0 = \mathrm{Wi_i}^2\left[\left\{1-\phi_1\,\mathrm{Wi_i}^2\sum_{k=1}^{\infty}\frac{k^{\alpha_t}}{\Lambda_{k,\mathrm{i}}^2}\right\}\sum_{k=1}^{\infty}\frac{k^{\alpha_t}}{\Lambda_{k,\mathrm{i}}^2}+\sum_{k=1}^{\infty}\frac{k^{\alpha_t}\left(k^{2\alpha_t}-3\,\mathrm{Wi_i}^2\right)}{\Lambda_{k,\mathrm{i}}^3}\right] \tag{194}$$

and where:

$$\phi_1 \equiv \frac{2(\lambda_2-\lambda_1)}{\lambda_1\sum_{k=1}^{\infty}\frac{k^{\alpha_t}+\frac{\lambda_2}{\lambda_1 k^{\alpha_t}}\mathrm{Wi_i}^2}{k^{2\alpha_t}+\mathrm{Wi_i}^2}} \tag{195}$$

$$\Lambda_{k,\mathrm{i}} \equiv k^{2\alpha_t}+\mathrm{Wi_i}^2 \tag{196}$$

Substituting her best-fit parameters into Eq. (194), and then solving by trial gives:

$$\mathrm{Wi_i} \equiv \lambda_1\dot{\gamma}_\mathrm{i} \approx 10.8 \tag{197}$$

and the corresponding value of η/η_0 is:

$$\frac{\eta_\mathrm{i}}{\eta_0} \equiv \frac{\eta(\dot{\gamma}_\mathrm{i})}{\eta_0} = 0.123 \tag{198}$$

Substituting Eqs. (188) and (189) into Eq. (32) yields:

$$\left.\frac{d\ln(\eta/\eta_0)}{d\ln(\lambda_1\dot{\gamma})}\right|_{\mathrm{Wi_i}} \equiv (n-1) = 2\left(\frac{\lambda_2}{\lambda_1}-1\right)\mathrm{Wi_i}\frac{\sum_{k=1}^{\infty}\frac{k^{\alpha_t}\,\mathrm{Wi_i}}{\left[k^{2\alpha_t}+\mathrm{Wi_i}^2\right]^2}}{\sum_{k=1}^{\infty}\frac{k^{\alpha_t}+\frac{\lambda_2}{\lambda_1}\frac{1}{k^{\alpha_t}}\mathrm{Wi_i}^2}{k^{2\alpha_t}+\mathrm{Wi_i}^2}} \equiv 2\left(\frac{\lambda_2}{\lambda_1}-1\right)\mathrm{Wi_i}\,\Sigma_\mathrm{R} \tag{199}$$

Substituting Eq. (199) into Eq. (43) gives:

$$m = \eta_0\frac{\eta_\mathrm{i}}{\eta_0}\left(\frac{\mathrm{Wi_i}}{\lambda_1}\right)^{-2\left(\frac{\lambda_2}{\lambda_1}-1\right)\mathrm{Wi_i}\,\Sigma_\mathrm{R}} \tag{200}$$

where Eq. (199) defines Σ_R. Substituting Eqs. (197), (198) and her best-fit parameters into Eq. (199) gives:

$$(n-1) = -0.629 \tag{201}$$

thus, the shear power-law index:

$$n = 0.371 \tag{202}$$

Substituting Eqs. (197), (198) and her best-fit parameters into Eq. (200) gives:

$$m = 551\ \mathrm{Pa\cdot s}^n \tag{203}$$

The first normal stress coefficient for multiple relaxation time is given by:

$$\Psi_1 = \sum_{k=1}^{\infty}\frac{1}{1+(\lambda_{1k}\dot{\gamma})^2}\Psi_{1k} \tag{204}$$

where, similarly to Eq. (180), we propose:

$$\Psi_{1k} = \frac{\Psi_{10}\lambda_{1k}}{\sum_k\lambda_{1k}} \tag{205}$$

and where λ_{1k} is defined by Eq. (181). Substituting Eq. (181) into Eq. (205) gives:

$$\Psi_{1k} = \frac{\Psi_{10}}{k^{\alpha_t}\sum_k\frac{1}{k^{\alpha_t}}} = \frac{\Psi_{10}}{k^{\alpha_t}\zeta(\alpha_t)} \tag{206}$$

where the Riemann zeta function is defined by Eq. (184). Substituting Eqs. (181) and (206) into Eq. (204) gives:

$$\Psi_1 = \frac{\Psi_{10}}{\zeta(\alpha_t)}\sum_{k=1}^{\infty}\frac{k^{\alpha_t}}{k^{2\alpha_t}+(\lambda_1\dot{\gamma})^2} \tag{207}$$

where:

$$\lim_{\lambda_1\dot{\gamma}\to 0}\Psi_1 = \frac{\Psi_{10}}{\zeta(\alpha_t)}\lim_{\lambda_1\dot{\gamma}\to 0}\sum_{k=1}^{\infty}\frac{k^{\alpha_t}}{k^{2\alpha_t}+(\lambda_1\dot{\gamma})^2} = \Psi_{10} \tag{208}$$

as it must, and where:

$$\lim_{\lambda_1\dot{\gamma}\to\infty}\Psi_1 = \frac{\Psi_{10}}{\zeta(\alpha_t)}\lim_{\lambda_1\dot{\gamma}\to\infty}\sum_{k=1}^{\infty}\frac{k^{\alpha_t}}{k^{2\alpha_t}+(\lambda_1\dot{\gamma})^2} = 0 \tag{209}$$

which implies that the curve does not inflect as it also must.

Adimensionalizing Eq. (207):

$$\frac{\Psi_1}{\Psi_{10}} = \frac{1}{\zeta(\alpha_t)}\sum_{k=1}^{\infty}\frac{k^{\alpha_t}}{k^{2\alpha_t}+(\lambda_1\dot{\gamma})^2} \tag{210}$$

and differentiating once gives:

$$\frac{d(\Psi_1/\Psi_{10})}{d(\lambda_1\dot{\gamma})} = \frac{-2(\lambda_1\dot{\gamma})}{\zeta(\alpha_t)}\sum_{k=1}^{\infty}\frac{k^{\alpha_t}}{\left(k^{2\alpha_t}+(\lambda_1\dot{\gamma})^2\right)^2} \tag{211}$$

or twice:

$$\frac{d^2(\Psi_1/\Psi_{10})}{d(\lambda_1\dot{\gamma})^2} = \frac{-2}{\zeta(\alpha_t)}\sum_{k=1}^{\infty}\frac{k^{\alpha_t}\left(k^{2\alpha_t}-3(\lambda_1\dot{\gamma})^2\right)}{\left(k^{2\alpha_t}+(\lambda_1\dot{\gamma})^2\right)^3} \tag{212}$$

Unlike the Carreau model, the first normal stress coefficient, $\Psi_1(\dot{\gamma})$, shares the same parameters with steady shear viscosity, η. She thus then inserts the parameters from Fig. 9 into Eq. (210), and then, in Fig. 10, compares Eq. (210) with the 32 first normal stress coefficient measurements from Fig. 4.3-6 of Bird *et al.* (1977). Fig. 10 illustrates this fit of the Oldroyd 8-constant model with $\eta_0 = 1100$ Pa·s, $\alpha_t = 2.7$, $\lambda_1 = 100$s and $\lambda_2 = 0.1$s [$\Psi_{10} = 2\eta_0(\lambda_1-\lambda_2) = 2.2\times10^5$ Pa·s^2]. From Fig. 10, we discover that the corotational Jeffreys model with multiple λ_1 and λ_2 (with parameters fitted in Fig. 9 [$\Psi_{10} = 2\eta_0(\lambda_1-\lambda_2) = 2.2\times10^5$ Pa·s^2]) and the data have different slopes. Substituting Eqs. (210)-(212) into Eq. (37) gives:

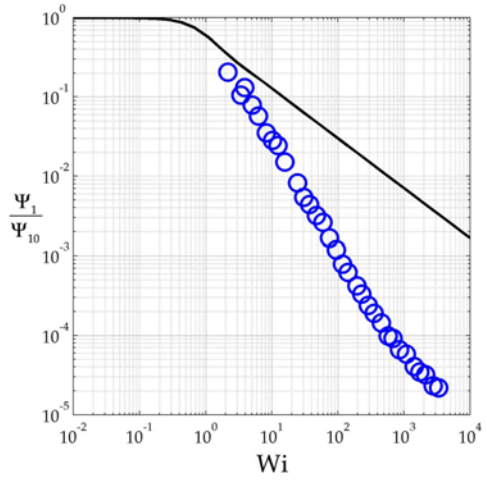

Fig. 10. Oldroyd 8-constant model (Black curve) [Eq. (210)] with parameters fitted in Fig. 9 [$\Psi_{10}=2\eta_0(\lambda_1-\lambda_2)=2.2\times10^5$ Pa·s^2] *versus* data from Fig. 4.3-6 of Bird *et al.* (1977) for 2.0% by weight polyisobutylene solution in Primol^{TM} white oil (Blue circles). The slopes differ.

$$\frac{d^2\ln(\Psi_1/\Psi_{10})}{d(\ln\lambda_1\dot\gamma)^2}=-2(\lambda_1\dot\gamma)^2\frac{\left[\sum_{k=1}^{\infty}\frac{k^{\alpha_t}}{k^{2\alpha_t}+(\lambda_1\dot\gamma)^2}+2(\lambda_1\dot\gamma)^2\sum_{k=1}^{\infty}\frac{k^{\alpha_t}}{\left(k^{2\alpha_t}+(\lambda_1\dot\gamma)^2\right)^2}\right]\sum_{k=1}^{\infty}\frac{k^{\alpha_t}}{\left(k^{2\alpha_t}+(\lambda_1\dot\gamma)^2\right)^2}}{\left(\sum_{k=1}^{\infty}\frac{k^{\alpha_t}}{k^{2\alpha_t}+(\lambda_1\dot\gamma)^2}\right)^2}$$
$$-2(\lambda_1\dot\gamma)^2\frac{\sum_{k=1}^{\infty}\frac{k^{\alpha_t}\left(k^{2\alpha_t}-3(\lambda_1\dot\gamma)^2\right)}{\left(k^{2\alpha_t}+(\lambda_1\dot\gamma)^2\right)^3}}{\sum_{k=1}^{\infty}\frac{k^{\alpha_t}}{k^{2\alpha_t}+(\lambda_1\dot\gamma)^2}} \tag{213}$$

Setting Eq. (213) to zero gives the inflection Weissenberg number, $\mathrm{Wi}_i\equiv\lambda_1\dot\gamma_i$:

$$0=\frac{\left[\sum_{k=1}^{\infty}\frac{k^{\alpha_t}}{k^{2\alpha_t}+\mathrm{Wi}_i^2}+2\,\mathrm{Wi}_i^2\sum_{k=1}^{\infty}\frac{k^{\alpha_t}}{\left(k^{2\alpha_t}+\mathrm{Wi}_i^2\right)^2}\right]\sum_{k=1}^{\infty}\frac{k^{\alpha_t}}{\left(k^{2\alpha_t}+\mathrm{Wi}_i^2\right)^2}}{\left(\sum_{k=1}^{\infty}\frac{k^{\alpha_t}}{k^{2\alpha_t}+\mathrm{Wi}_i^2}\right)^2}+\frac{\sum_{k=1}^{\infty}\frac{k^{\alpha_t}\left(k^{2\alpha_t}-3\,\mathrm{Wi}_i^2\right)}{\left(k^{2\alpha_t}+\mathrm{Wi}_i^2\right)^3}}{\sum_{k=1}^{\infty}\frac{k^{\alpha_t}}{k^{2\alpha_t}+\mathrm{Wi}_i^2}} \tag{214}$$

Substituting her best-fit parameters into Eq. (214), and then solving by trial gives:

$$\mathrm{Wi}_i\equiv\lambda_1\dot\gamma_i\approx12.6 \tag{215}$$

and the corresponding value of Ψ_{1i}/Ψ_{10} is:

$$\frac{\Psi_{1i}}{\Psi_{10}}\equiv\frac{\Psi_1(\dot\gamma_i)}{\Psi_{10}}=0.111 \tag{216}$$

Substituting Eqs. (210) and (211) into Eq. (36) gives:

$$\frac{d\ln(\Psi_1/\Psi_{10})}{d\ln(\lambda_1\dot\gamma)}=-2\,\mathrm{Wi}^2\frac{\sum_{k=1}^{\infty}\frac{k^{\alpha_t}}{\left(k^{2\alpha_t}+(\lambda_1\dot\gamma)^2\right)^2}}{\sum_{k=1}^{\infty}\frac{k^{\alpha_t}}{k^{2\alpha_t}+(\lambda_1\dot\gamma)^2}} \tag{217}$$

Taking the limit as $\lambda_1\dot\gamma\to\infty$ gives the asymptote slope of the curve:

$$\frac{d\ln(\Psi_1/\Psi_{10})}{d\ln(\lambda_1\dot\gamma)}=(n'-2)=-2 \tag{218}$$

which matches the result for single relaxation time, Eq. (218). Substituting Eq. (131) into Eq. (44) gives:

$$m'=\Psi_{10}\frac{\Psi_{1i}}{\Psi_{10}}\left(\frac{\mathrm{Wi}_i}{\lambda_1}\right)^2 \tag{219}$$

Substituting $\Psi_{10}=2.2\times10^5$ Pa·s^2, Eqs. (215) and (216) into Eq. (219) gives:

$$m'=387.\ \mathrm{Pa}\cdot\mathrm{s}^{n'} \tag{220}$$

She then calculates the first inflection pairing time, λ_B'. Substituting $n'=0$, Eqs. (202), (203) and (220) into Eq. (4) gives:

$$\lambda_B'\equiv\left(\frac{387.}{2(551.)}\right)^{-1/0.370}=16.9\,\mathrm{s} \tag{221}$$

She finally calculates the Leider number, Ld. Substituting $t_p=100\,\mathrm{s}$, Eqs. (202) and (221) into Eq. (165) gives:

$$\mathrm{Ld}\approx\frac{0.371(16.9\,\mathrm{s})}{100\,\mathrm{s}}=0.063<1 \tag{222}$$

thus, she can expect her quasi-steady state solution to apply. This conclusion for the Oldroyd 8-constant model matches the conclusion from Worked Example 5.1 for the Carreau model.

Acknowledgments

This research was undertaken, in part, thanks to funding from the Canada Research Chairs program of the Government of Canada for the Natural Sciences and Engineering Research Council of Canada (NSERC) Tier 1 Canada Research Chair in Rheology. The financial support of the Royal Golden Jubilee Program of the Thailand Research Fund for (Contract No. PHD/0116/2554) is also greatly appreciated. A.J. Giacomin is indebted to the Faculty of Applied Science and Engineering of Queen's University at Kingston, for its support through a Research Initiation Grant (RIG).

References

Abramowitz, M. and I.A. Stegun, 1970, *Handbook of mathematical functions-with formulas, graphs, and mathematical tables*, National Bureau of Standards, Washington DC.

Baird, D.G. and D.I. Collias, 1998, *Polymer processing: principles and design*, John Wiley & Sons, New York.

Baird, D.G. and D.I. Collias, 2014, *Polymer processing: principles and design*, 2nd ed., John Wiley & Sons, New York.

Bird, R.B., R.C. Armstrong, and O. Hassager, 1977, *Dynamics of*

Polymeric Liquids, Vol. 1, 1st ed., Wiley, New York.

Bird, R.B., R.C. Armstrong, and O. Hassager, 1987, *Dynamics of Polymeric Liquids*, Vol. 1, 2nd ed., Wiley, New York.

Bird, R.B., W.E. Stewart, and E.N. Lightfoot, 2007, *Transport Phenomena*, Revised 2nd ed., Wiley & Sons, New York.

Bird, R.B., W.E. Stewart, E.N. Lightfoot, and D.J. Klingenberg, 2015, *Introductory Transport Phenomena*, Wiley & Sons, New York.

Camilleri, C.J. and J.R. Jones, 1966, The effect of a pressure gradient on the secondary flow of non-Newtonian liquids between non-intersecting cylinders, *Zeitschrift für angewandte Mathematik und Physik* **17**, 78-90.

Huppler, J.D., E. Ashare, and J.A. Holmes., 1967, Rheological properties of three solutions. Part I. Non-Newtonian viscosity, normal stresses, and complex viscosity, *Transac. Soc. Rheo.* **11**, 159-179.

Jeffreys, H., 1924, *The Earth: Its Origin, History and Physical Constitution*, Cambridge, London.

Jeffreys, H., 1929, *The Earth: Its Origin, History and Physical Constitution*, 2nd ed., Cambridge, London.

Jones, J.R., 1964, Flow of elastic-viscous liquids in pipes with cores (Part I), *J. Mécanique* **3**, 79-99. Errata: In Eqs. (20) and (22a), "*a* const.," should be "a const.,"; In Eq. (15), "$9\sigma_2 \geq \sigma_1 \geq 1$" should be "$9\sigma_2 \geq \sigma_1 \geq 1$"; In Eq. (45), "$\boldsymbol{w}' = \boldsymbol{w}_0 + (1-\sigma)S\boldsymbol{w}_1 + S^2\boldsymbol{w}_2 + S^3\boldsymbol{w}_3 + \ldots$" should be "$\boldsymbol{w}' = \boldsymbol{w}_0 + (1-\sigma)S\boldsymbol{w}_1 + (1-\sigma)^2 S^2\boldsymbol{w}_2 + (1-\sigma)^3 S^3\boldsymbol{w}_3 + \ldots$"; In Eq. (54), "$\psi_n =$" should be "$\Psi_n =$"; In Eq. (3.5), "$\omega_{ij} =$" should be "$\omega_{ik} =$"; In Eq. (16), "$Z^* = x + iy$" should be "$Z^* = x - iy$."; The first term on RHS of Eq. (23) "γ_2" should be "γ^2"; The expression for $F_1^{(4)}$ in Eq. (56), "r^{-4}" should be "r–4".

Jones, J.R., 1965, Flow of elastico-viscous liquids in pipes with cores (Part II), *J. Mécanique* **4**, 121-132.

Jones, J.R. and R.S. Jones, 1966, Flow of elastico-viscous liquids in pipes with Cores (Part III), *J. Mécanique* **5**, 375-395.

Jones, R.S., 1967, Flow of an elastico-viscous liquid in a corrugated pipe, *J. Mécanique* **6**, 443-448.

Leider, P.J., 1974, Squeezing flow between parallel disks. II. Experimental results, *Ind. Eng. Chem. Fund.* **13**, 342-346.

Leider, P.J. and R.B. Bird, 1974, Squeezing flow between parallel disks. I. Theoretical analysis, *Ind. Eng. Chem. Fund.* **13**, 336-341.

Oldroyd, J.G., 1958, Non-Newtonian effects in steady motion of some idealized elastico-viscous liquids, *Proc. Roy. Soc. London* **245**, 278-297.

Saengow, C., A.J. Giacomin, and C. Kolitawong, 2015a, Extruding plastic pipe from eccentric dies, *J. Non-Newton. Fluid Mech.* **223**, 176-199.

Saengow, C., A.J. Giacomin, and C. Kolitawong, 2015b, *Extruding Plastic Pipe from Eccentric Dies, PRG Report No.011*, QU-CHEE-PRG-TR--2015-11, Polymers Research Group, Chem. Eng. Dept., Queen's University, Kingston, Canada.